ARTICLES

Thyrotrophin in the pars tuberalis triggers photoperiodic response

Nobuhiro Nakao[1]*, Hiroko Ono[1]*, Takashi Yamamura[1], Tsubasa Anraku[1], Tsuyoshi Takagi[1], Kumiko Higashi[1], Shinobu Yasuo[1], Yasuhiro Katou[1], Saburo Kageyama[1], Yumiko Uno[1], Takeya Kasukawa[2], Masayuki Iigo[3], Peter J. Sharp[4], Atsushi Iwasawa[5], Yutaka Suzuki[6], Sumio Sugano[6], Teruyuki Niimi[7], Makoto Mizutani[8], Takao Namikawa[8], Shizufumi Ebihara[1,8], Hiroki R. Ueda[2,9] & Takashi Yoshimura[1,8,10]

Molecular mechanisms regulating animal seasonal breeding in response to changing photoperiod are not well understood. Rapid induction of gene expression of thyroid-hormone-activating enzyme (type 2 deiodinase, *DIO2*) in the mediobasal hypothalamus (MBH) of the Japanese quail (*Coturnix japonica*) is the earliest event yet recorded in the photoperiodic signal transduction pathway. Here we show cascades of gene expression in the quail MBH associated with the initiation of photoinduced secretion of luteinizing hormone. We identified two waves of gene expression. The first was initiated about 14 h after dawn of the first long day and included increased thyrotrophin (TSH) β-subunit expression in the pars tuberalis; the second occurred approximately 4 h later and included increased expression of *DIO2*. Intracerebroventricular (ICV) administration of TSH to short-day quail stimulated gonadal growth and expression of *DIO2* which was shown to be mediated through a TSH receptor–cyclic AMP (cAMP) signalling pathway. Increased TSH in the pars tuberalis therefore seems to trigger long-day photoinduced seasonal breeding.

Animals living outside the tropics use changes in photoperiod to adapt to seasonal changes in environment, but the molecular mechanisms underlying photoperiodic time measurement are not fully understood[1]. The Japanese quail is a robust model for the study of these mechanisms because of its rapid and dramatic response to changes in photoperiod. When quail are transferred from short to long days, plasma luteinizing hormone increases at the end of the first long day: this photoperiodic response is the core feature of the avian 'first day release model' of reproductive photoperiodism[2,3]. In birds, the components required for photoperiodic signal transduction are located in the mediobasal hypothalamus (MBH) and include a deep brain photoreceptor[4], a clock to measure daylength[5], and output pathways to regulate the secretion of gonadotrophin-releasing hormone (GnRH)[6,7]. Recently, we have reported that long-day-induced local activation of thyroid hormone metabolism in the quail MBH is an early event in photoperiodic signal transduction[8,9]. Under short-day conditions, expression of type 2 deiodinase (*DIO2*), which converts the prohormone thyroxine (T_4) to bioactive triiodothyronine (T_3), is maintained at a low level, whereas expression of type 3 deiodinase (*DIO3*), which metabolizes T_4 and T_3 to reverse (r)T_3 and T_2, respectively, is maintained at a high level. When quail are transferred from short to long days, rapid reciprocal switches in *DIO2* and *DIO3* expression occur at the end of the first long day, resulting in a local increase in T_3 concentration. This increase in MBH T_3 concentration precedes the first rise in the concentration of photoinduced plasma luteinizing hormone and is causally related. Administration of T_3 to short-day quail stimulates secretion of luteinizing hormone and testicular growth, whereas conversely, administration of a DIO2 inhibitor inhibits photoinduced testicular growth[8,10]. The question now is the identity of the photoperiodic transduction pathway regulating *DIO2* expression in the MBH.

To address this, we have dissected the molecular dynamics of gene expression regulating photoinduced thyroid hormone metabolism in the quail MBH during the first day of photoinduced luteinizing hormone secretion by using a chicken high-density oligonucleotide microarray. Quail and chicken are both galliforms with predicted high interspecific DNA sequence conservation. To test this prediction, we applied biotinylated chicken and quail genomic DNA to the array. Signals for 82.2% of the probes were statistically indistinguishable between the two species (Welch's *t*-test, Benjamini and Hochberg false discovery rate (FDR) multiple test, $P > 0.05$, $n = 3$) (Supplementary Fig. 1).

Genome-wide expression analysis

To study changes in gene expression during the first long day, eight-week-old male quail kept under short days (6/18 h light/dark cycle) for four weeks were transferred to long days (20/4 h light/dark cycle). Plasma samples and brains were collected from six birds every 4 h for three days during this transition. In addition, samples were collected every 2 h between 10 and 22 h after dawn of the first long day to cover the period during the initiation of the photoperiodic response when the most rapid changes in gene expression were predicted to occur[2,3]. The first increase in plasma luteinizing hormone was observed at 22 h after dawn of the first long day as previously reported[3,11] (Fig. 1a)

[1]Division of Biomodelling, Graduate School of Bioagricultural Sciences, Nagoya University, Furo-cho, Chikusa-ku, Nagoya 464-8601, Japan. [2]Functional Genomics Subunit, Centre for Developmental Biology, RIKEN, 2-3-3 Minatojima-minamimachi, Chuo-ku, Kobe 650-0047, Japan. [3]Department of Applied Biochemistry, Faculty of Agriculture, Utsunomiya University, 350 Mine-machi, Utsunomiya, 321-8505, Japan. [4]Division of Genetics and Genomics, Roslin Institute and Royal (Dick) School of Veterinary Studies, University of Edinburgh, Roslin, Midlothian EH25 9PS, UK. [5]Laboratory of Comparative Biochemistry, Graduate School of Applied Biological Sciences, Gifu University, Gifu 501-1193, Japan. [6]Department of Medical Genome Sciences, Graduate School of Frontier Sciences, University of Tokyo, 4-6-1 Shirokanedai, Minato-ku, Tokyo 108-8639, Japan. [7]Division of Biofunctions Development, Graduate School of Bioagricultural Sciences, Nagoya University, Furo-cho, Chikusa-ku, Nagoya 464-8601, Japan. [8]Avian Bioscience Research Centre, Graduate School of Bioagricultural Sciences, Nagoya University, Furo-cho, Chikusa-ku, Nagoya 464-8601, Japan. [9]Laboratory for Systems Biology, Centre for Developmental Biology, RIKEN, 2-3-3 Minatojima-minamimachi, Chuo-ku, Kobe 650-0047, Japan. [10]Institute for Advanced Research, Nagoya University, Furo-cho, Chikusa-ku, Nagoya 464-8601, Japan. *These authors contributed equally to this work.

(one-way analysis of variance (ANOVA), $F_{20,105} = 5.860$, $P < 0.0001$, Fisher's least significant difference (LSD) post-hoc test, $P < 0.05$, $n = 6$).

For each time point, biotinylated antisense RNAs (cRNAs) prepared from pooled MBH were hybridized to duplicate sets of arrays to minimize experimental error. Using the RMA algorithm and statistical cosine filters[12], we identified 77 cycling genes which were disqualified from consideration as long-day-induced genes (Fig. 1b and Supplementary Table 1). These genes included eight circadian clock genes (Supplementary Fig. 2). We next focused on genes showing 1.5-fold or more changes in expression during the first long day, and found two waves of expression initiated at around 14 h (peak time 16.46 h, Fig. 1a) and the other initiated at around 18 h after dawn (peak time 21.15 h, Fig. 1a) (Supplementary Table 2 and Supplementary Fig. 3) (Welch's one-way ANOVA, FDR $P < 0.01$).

The first wave comprised two genes encoding thyrotrophin-β (TSH-β) and eyes absent 3 (EYA3); the second wave comprised 11 genes including *DIO2* and *DIO3* which showed inversely related changes in expression (Supplementary Fig. 4). Using *in situ* hybridization, the expression of the two first-wave genes (*TSHB* and *EYA3*) was observed in the pars tuberalis of the pituitary gland, whereas expression of six of the second-wave genes including *DIO2* and *DIO3* was observed in the ependymal cells lining the ventro-lateral walls of third ventricle and in the adjacent infundibular nucleus (Fig. 1c).

We also noted rhythmic expression of the gene encoding common pituitary glycoprotein alpha subunit (CGA) in the pars tuberalis (Fig. 1c and Supplementary Fig. 2). The expression of this gene with that encoding the TSH-β suggests that the proteins encoded by these genes associate in the pars tuberalis to form TSH. This view is supported by the observation that TSH-β protein occurs in pars tuberalis cells (Fig. 2a). We therefore deduced that increased TSH in the pars tuberalis may be functionally significant for photoperiodic signal transduction. To test this hypothesis, we first determined whether TSH receptor (*TSHR*) gene expression occurs in the MBH.

TSH receptor in the MBH

Strong expression of *TSHR* was observed in the ependymal cells and pars tuberalis; weak expression was observed in the infundibular nucleus (Fig. 2b). *TSHR* expression in the pars tuberalis was detected at 6 and 22 h after dawn of the first long day but not at 14 h, whereas it occurred in the ependymal cells all the times examined ($n = 2$). To verify these results, we further performed a ^{125}I-labelled TSH binding assay. We first demonstrated specific binding of ^{125}I-labelled TSH in the thyroid gland of quail as a positive control (Fig. 2c). Specificity of the binding assay was also confirmed by radioreceptor assay (Supplementary Fig. 5). We then observed specific binding of ^{125}I-labelled TSH in the ependymal cells, infundibular nucleus and the pars tuberalis. This observation is consistent with expression sites of *TSHR* mRNA at these loci. Although TSH binding in the ependymal cells was observed at all the times examined, that in the pars tuberalis was undetectable at time 22 h (Fig. 2d). Because the median eminence is one of the circumventricular organs and is outside the blood–brain barrier[13], long-day-induced TSH in the pars tuberalis has the potential to enter the brain to interact with TSHR in the ependymal cells and infundibular nucleus. We therefore predicted that the

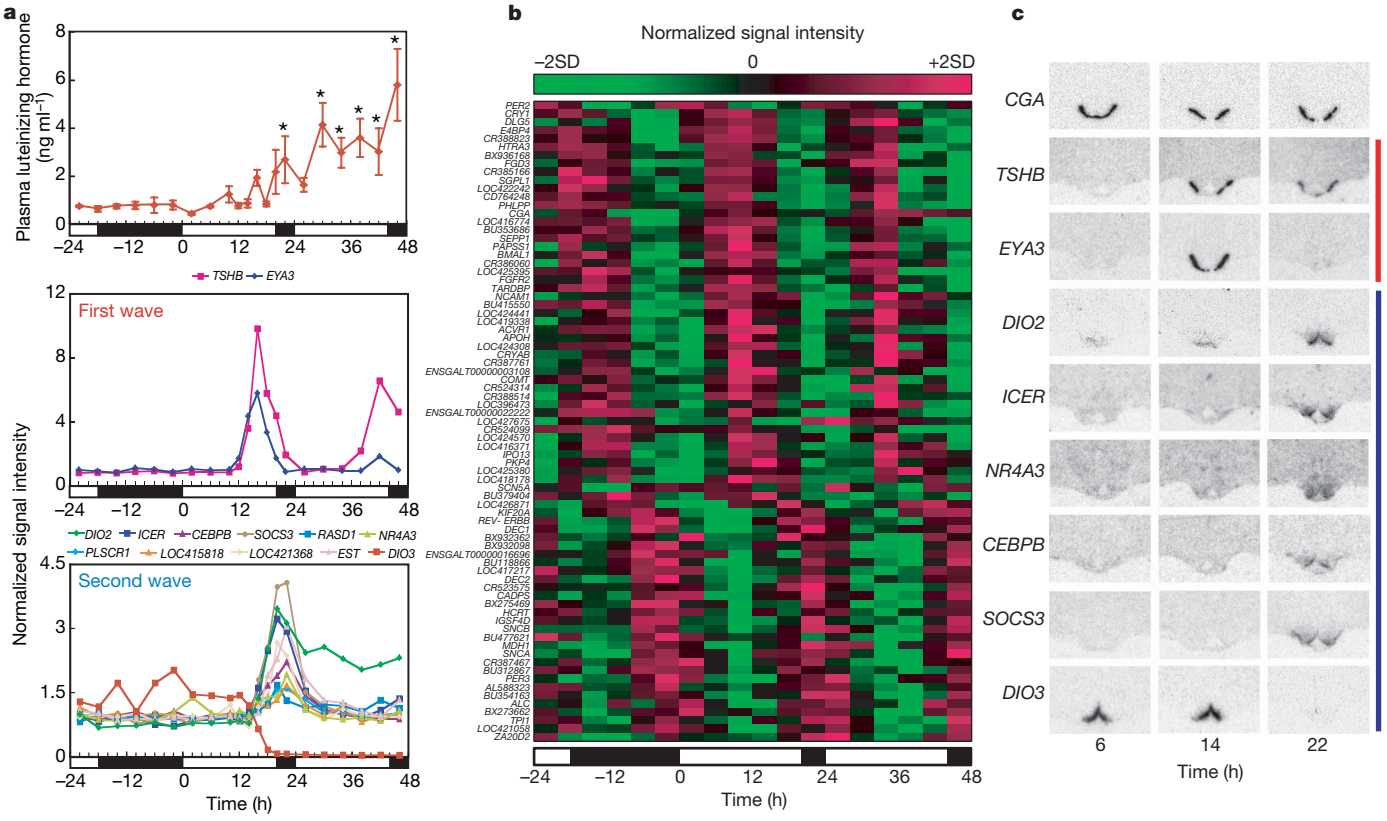

Figure 1 | Plasma luteinizing hormone and genome-wide analysis of genes expressed in the quail MBH during the first day of photostimulation (time 0 h is dawn of the first long day). **a**, Changes in plasma luteinizing hormone (mean ± s.e.m., $n = 6$, $^*P < 0.05$ versus the value at time −22 h); and timing of first- and second-wave gene expression. Data are normalized such that the median signal strength for each gene over all time points was 1.0. The average signal strength at each point was then displayed as a ratio relative to the median signal strength of that gene. **b**, Organization of 77 genes showing 24 h rhythmic changes in expression. Data are normalized such that the mean and s.d. of log expression values over all time points for each gene are 0 and 1, respectively. Italic script, gene identities and accession numbers. **c**, Spatio-temporal expression of common glycoprotein hormone subunit (*CGA*), first-wave (red bar) and second-wave genes (blue bar). Expression of *CGA* and first-wave genes was observed in the pars tuberalis, whereas that of second-wave genes was observed in the ependymal cells and the infundibular nucleus.

photoinduced increase in pars tuberalis TSH may function to stimulate the expression of *DIO2* and possibly other second-wave genes.

TSH regulation of *DIO2* gene

To test this prediction, a range of doses (0.01, 0.1, 1.0 mIU) of bovine TSH[14] dissolved in 10 µl saline was administered 16 h after dawn to short-day quail to correspond with the time that *TSHB* expression is at its highest in the pars tuberalis after dawn of a first long day. Brains were collected 4 h after the injection when the induction of second-wave genes was predicted to be maximal. As shown in Fig. 3a, b, intracerebroventricular (ICV) TSH injection induced the expression of the *DIO2* and three other second-wave genes in a dose-dependent manner (one-way ANOVA, Fisher's LSD post-hoc test, $P < 0.05$, $n = 3$–6). Induction of these genes was observed in the dorsal and ventrolateral ependymal cells and in the infundibular nucleus (Figs 3a and 5a) and was more prominent in the ependymal cells than in photostimulated birds (Fig. 1c and Supplementary Fig. 6). This is likely to be a consequence of the periventricular ependymal cells being more assessable to ICV TSH than to TSH originating from the pars tuberalis. We further confirmed this physiological effect of TSH by ICV injection of TSH-β antibody to long-day quail. Anti-chicken/quail TSH-β IgG[15] or pre-immune serum IgG (1 µg per 10 µl) was administered every 2 h (ref. 16) from 12 h to 18 h after dawn of the first long day, and brains were collected 2 h after the last injection. As shown in Fig. 3c, d, anti-TSH-β IgG injections suppressed the expression of the four second-wave genes, including *DIO2*, shown to be induced by ICV TSH.

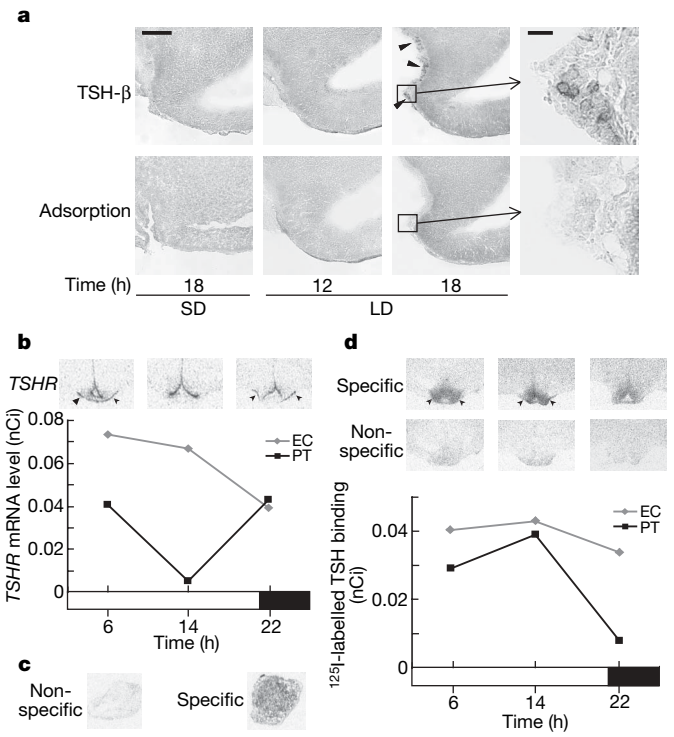

Figure 2 | Localization of TSH-β and TSHR in the pars tuberalis and MBH. **a**, Positive immunolabelling for TSH-β in the pars tuberalis (arrowhead) induced by the long-day stimulus was eliminated by pre-adsorption of the anti-TSH-β antibody with the synthetic TSH-β peptide sequence used to produce the antibody. Scale bars: left, 100 µm; right, 10 µm. SD, short day; LD, long day. **b**, Expression of *TSHR* mRNA in the ependymal cells was observed at all the times examined, whereas that in the pars tuberalis (arrowhead) was not observed at time 14 h ($n = 2$). **c**, **d**, Binding of ^{125}I-labelled TSH to quail thyroid gland (**c**) and the MBH (**d**). Although TSH binding in the ependymal cells and the infundibular nucleus was observed at all the times examined, that in the pars tuberalis was not observed at time 22 h ($n = 2$).

Involvement of cyclic AMP signalling pathway

To further address the mechanism through which TSH might regulate the expression of *DIO2* and three other second-wave genes we first determined the transcriptional start sites using the oligo-capping method[17] and mapped them to quail and chicken genome sequences (Fig. 4a, Supplementary Fig. 7a). It is reported that the expression of *DIO2* in human thyroid gland is regulated through a TSHR-Gsα-cAMP regulatory cascade[18]. We found several putative cAMP responsive elements (CREs) in the 1.5 kilobase (kb) 5′ upstream regions of *DIO2*, in quail and chicken (Fig. 4a) and in the three other second-wave genes (Supplementary Fig. 7a). Conservation of CREs between the two species suggests the functional significance of this element (Fig. 4b and Supplementary Fig. 7b). To validate whether these CREs are involved in the regulation of *DIO2* gene by TSH, we analysed the promoter activity of the *DIO2* gene transfected into the 293 cell line. TSH administration induced expression of *DIO2* reporter activity in a dose-dependent manner only when *TSHR* was co-transfected (Supplementary Fig. 8). However, when CREs were mutated, induction by TSH was not observed (Fig. 4c). These results demonstrate that induction of the *DIO2* gene by TSH involves a cAMP signalling pathway through TSHR.

Photoperiodically regulated output genes

We next performed a microarray analysis on quail kept under short- and long-day conditions for two weeks to assess the chronic effects of photostimulation on MBH gene expression. MBH samples were collected from six birds every 4 h during a 24 h lighting cycle. This analysis identified 183 differentially expressed genes (Welch's two way ANOVA, FDR $P < 0.05$) (Supplementary Fig. 9a, b and Supplementary Table 3). Among these genes, 124 were upregulated and 59 were downregulated under long-day conditions (Supplementary

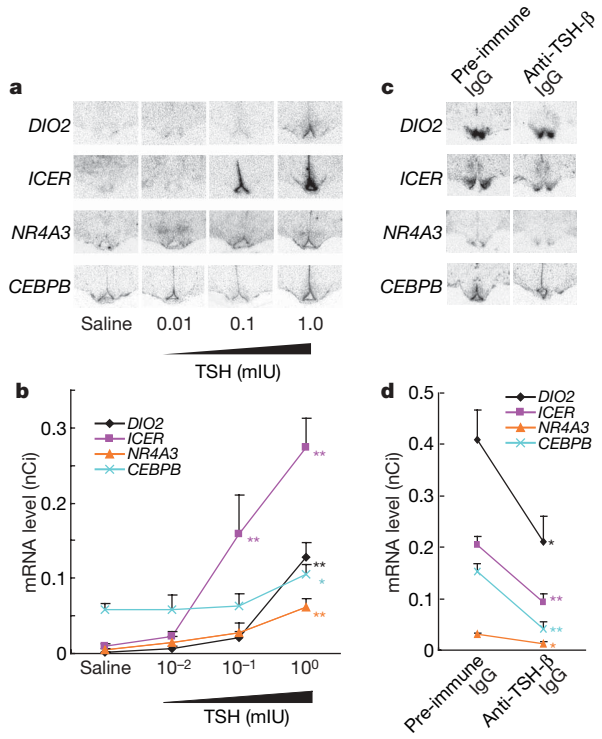

Figure 3 | Induction of the expression of *DIO2* and three other second-wave genes by ICV injection of TSH and inhibition by ICV injection of anti-TSH-β IgG. ICV injection of TSH (**a**, **b**) and anti-TSH-β IgG (**c**, **d**). Representative autoradiograms (**a**, **c**) and densitometric quantification (**b**, **d**) showing the effect of ICV injections of TSH/anti-TSH-β (**b**, $*P < 0.05$, $**P < 0.01$, ANOVA, Fisher's LSD post-hoc test, $n = 3$–6; **d**, $*P < 0.05$, $**P < 0.01$, *t*-test, mean + s.e.m., $n = 3$).

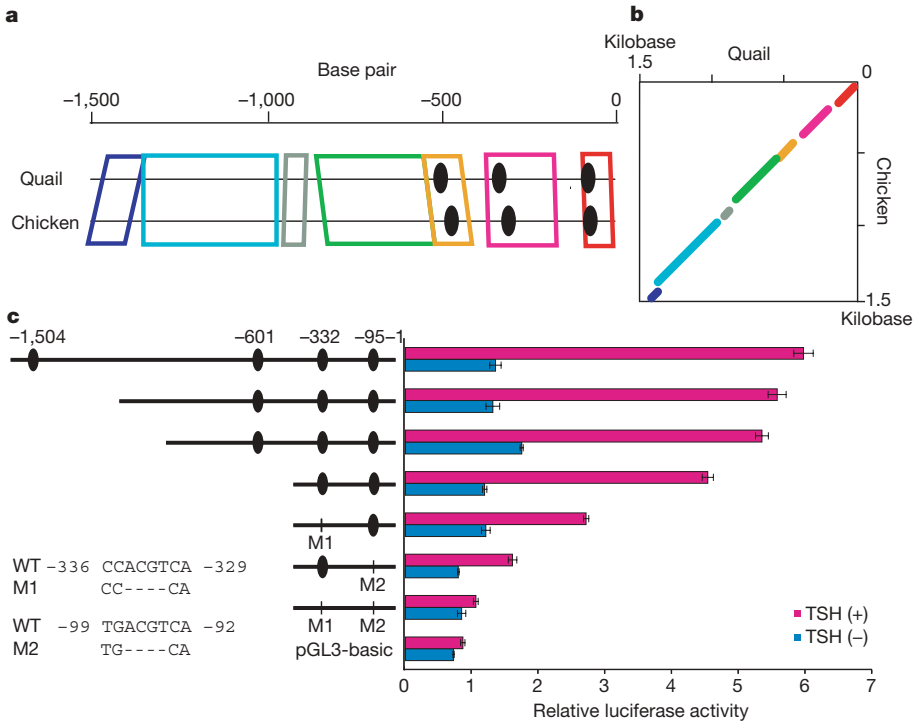

Figure 4 | Involvement of a cAMP signalling pathway in TSH induction of *DIO2* gene expression. **a**, Comparison of quail and chicken *DIO2* gene 5′ upstream sequences. Conserved segments are boxed. Filled ovals, putative CRE sites. **b**, Dot plot analysis of 5′ upstream regions using BLASTN, with greater than 85% identity. **c**, Promoter activity of quail *DIO2*. Wild-type and deletion/mutant reporters fused to the luciferase gene were assayed for their activities in response to TSH. Each value represents the mean ± s.e.m. of three replicates for a single assay.

Fig. 9a, b). We found long-day-induced expression of *DIO2* and reduced expression of *DIO3*, as previously reported[8,9] (Supplementary Fig. 10). *In situ* analysis of genes with known functions and showing differences in expression between long and short days, in the MBH, other than *DIO2* and *DIO3*, confirmed the microarray analysis (Supplementary Fig. 9c). In addition, we found a set of genes encoding various hormones and hormone receptors, which included *TSHB* and *CGA* (Supplementary Fig. 10 and Supplementary Table 3). Because high expression of *TSHB* and *CGA* was observed under chronic long-day conditions, we deduced that increased pars tuberalis TSH may not only play a role in initiating photoinduced secretion of luteinizing hormone, but may also be necessary to maintain the expression of other genes required to support a full reproductive response. We therefore investigated this possibility by prolonged ICV infusion of TSH (1.2 mIU per day) in short-day quail between 8 and 10 weeks of age. This treatment simulated MBH *DIO2* expression and gonadal development (Fig. 5).

Discussion

We have used the 'first day release model' of photoinduced luteinizing hormone release in quail to dissect the temporal pattern of changes in gene expression in the MBH associated with the initiation of photoinduced reproductive function. We found 77 genes that displayed a temporal pattern of expression under short and long days that would be expected of clock genes or clock-driven genes. Because most cycling genes are tissue specific[12,19], future analyses of the relations between the functions of these genes are likely to reveal further details of the molecular basis of the photoperiodic response. Our most important observation was the photoinduction of a first wave of gene expression initiated about 14 h after dawn of the first long day, comprising *TSHB* and *EYA3* in the pars tuberalis. These changes in gene expression are the earliest yet reported, to our knowledge, for the photoperiodic signal transduction pathway. This was followed approximately 4 h later by a second wave of gene expression in the ependymal cells and infundibular nucleus and included an increase in *DIO2*, a key element in the photoperiodic signal transduction pathway[8]. EYA3 is a transcriptional co-activator involved in the development of the eye and forms a nuclear complex with SIX (sine oculis) DNA-binding homeodomain factor and DACH (dachshund) nuclear cofactors[20]; we considered the possibility that the photoinduction of *EYA3* may induce expression of second-wave genes. However, this is unlikely because if *EYA3* is involved in second-wave gene expression it would need to be co-localized with these genes to exert its function. In the present study, *EYA3* was expressed in the pars tuberalis whereas second-wave genes were expressed in the ependymal cells and infundibular nucleus. Several *SIX* genes were observed in the pars tuberalis (Supplementary Fig. 11), suggesting that these may interact with long-day-induced *EYA3* to regulate the expression of genes, the identity of which remains to be established. We therefore focused on the possibility that *TSHB* in the pars tuberalis might be involved in the initiation of *DIO2* and the expression of other second-wave genes. Among the various cycling genes, we found rhythmic expression of *CGA*, and the peak of *CGA* preceded that of

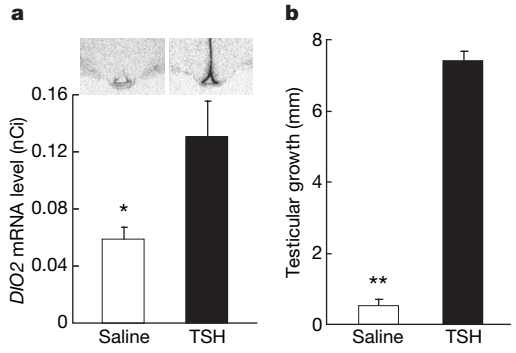

Figure 5 | Effect of chronic ICV infusion of TSH on MBH *DIO2* expression and testicular growth under short-day conditions. **a**, MBH *DIO2* expression. **b**, Testicular growth. (*$P < 0.05$, **$P < 0.01$, *t*-test, mean + s.e.m. $n = 5$).

long-day-induced *TSHB*. The biological activity of TSH requires a non-covalent association of CGA and TSH-β[21]. Thus it appears that the cycling CGA is available for dimerization with long-day-induced TSH-β to form bioactive TSH. It is also of note that translation of TSH occurs at least within 20 min[21]. In addition, unlike luteinizing hormone, dimerization of TSH-β and CGA, and secretion of TSH is very rapid and efficient, with a value of $t_{1/2}$ for the intracellular disappearance (that is secretion) of about 1 h (ref. 21). The expression of *CGA* and *TSHB* in the pars tuberalis therefore indicates that this is a source of biologically active TSH which may be transported into the third ventricle, possibly through tanycytes which abut the pars tuberalis[22]. The target site for pars tuberalis TSH was suggested by the presence of *TSHR* gene expression in the ependymal cells, infundibular nucleus and the pars tuberalis. This observation was supported by a ^{125}I-labelled TSH binding assay which showed specific TSH binding in these loci. Observations on the effects of ICV injection of TSH and anti-TSH-β IgG on *DIO2* and three other second-wave genes demonstrated that TSH triggers the expression of these genes in the ependymal cells. Furthermore, promoter analysis indicated that the induction of *DIO2* is likely to be mediated by the cAMP-signalling pathway. This observation is consistent with the action of TSH on human thyroid gland and rat brown adipose tissue, where *DIO2* expression is regulated by a TSHR–cAMP mediated mechanism[18,23]. Our study revealed a similar TSHR–cAMP mediated mechanism in the quail MBH. In addition to the acute effect of ICV TSH, chronic administration of TSH maintained increased *DIO2* expression and induced testicular growth under short-day conditions. This suggests that elevated TSH in the pars tuberalis may be required to maintain photoinduced reproductive function.

Although it is known that several species become photoperiodically blind after thyroidectomy, quail can respond to photoperiod even after thyroidectomy[1]. Recently, we have reported the involvement of TGF-α in the photoperiodism, and that the TGF-α signalling pathway is not dependent on thyroid hormone activity[24]. Interestingly, the similarity in expression profile between *DIO2* and *TGF-α* suggested that these two genes share the same transcriptional regulation. Although we failed to detect *TGF-α* gene expression in the present microarray analysis, we found TSH induced expression of *TGF-α* (Supplementary Fig. 12a, b). It is, therefore, possible that pars tuberalis TSH may signal photoperiodic information through both DIO2 and TGF-α. The magnitude of testicular growth induced by ICV TSH administration in short-day quail was indistinguishable from that of intact birds kept under long-day conditions (Supplementary Fig. 12c). This suggests that TSH is important not only for triggering photoperiodic responses, but also for the maintaining photoperiodically induced reproductive neuroendocrine function.

Since the discovery of dense melatonin receptors in the pars tuberalis in most mammalian species, but not birds, the pars tuberalis in mammals is considered to be involved in the transmission of photoperiodic stimuli to endocrine outputs through melatonin[25,26]. Further, the thyrotrophe cell type in the mammalian pars tuberalis expresses a high density of melatonin receptors and may regulate seasonal prolactin secretion[27]. However, unlike mammals, there is no evidence that circulating melatonin plays a role in photoperiodic transduction in birds[28]. Consequently, the mechanism transducing photoperiodic information to the avian pars tuberalis remains to be discovered. However, pars tuberalis TSH may be an evolutionarily conserved element of a photoperiodic signal transduction pathway in birds and mammals. This view is consistent with an earlier finding in sheep that expression of TSH-β in the pars tuberalis is not regulated by classical thyrotrophe receptors and their intracellular pathways, but through a novel, photoperiod-dependent mechanism[29].

Our view that photoinduced pars tuberalis TSH in the quail enters the cerebrospinal fluid to induce a photoperiodic response is consistent with the finding in the hamster that photoperiod-dependent changes in TSH-like immunoreactivity occur in the pars tuberalis[30] whereas TSH is found in the cerebrospinal fluid and central nervous system (CNS) of mammals[31,32]. The expression of *TSHR* has been reported in the mammalian brain[33,34], but no function has been proposed in relation to the control of photoperiodic responsiveness. In the present study, we show that long-day-induced TSH in the pars tuberalis triggers the expression of *DIO2* in the ependymal cells (Supplementary Fig. 13). To our knowledge, this is the first demonstration of the likely functional significance of pars-tuberalis-derived TSH in the CNS. Recently, it has been proposed that the pars tuberalis in sheep may be the circannual pacemaker for seasonal prolactin secretion[35]. Thus, the pars tuberalis appears to be the locus for the control of seasonality both in birds and other vertebrates.

In conclusion, one of the most important questions in photoperiodism is the identity of the molecular basis of the mechanism underlying the photoinducible phase that in the quail occurs 12–16 h after dawn[2]. Because photoinduction of *TSHB* expression was observed from about 12 h after dawn of the first long day, increased *TSHB* expression in the pars tuberalis may be the key molecular event defining the onset of the photoinducible phase. Our study presents the first comprehensive analysis of changes in hypothalamic gene expression likely to be involved in the regulation of the long-day reproductive photoperiodic response, and identifies pars tuberalis TSH as a key factor controlling photoperiodic signal transduction. The identification of a key role for *TSHB* expression in the pars tuberalis in reproductive photoperiodic time measurement marks a major advance in our knowledge of molecular mechanisms controlling seasonal breeding.

METHODS SUMMARY

Animals. We used Japanese quail (*C. japonica*) obtained from a local dealer and chicken (*Gallus domesticus*) (WL-G) kept in our colony. Because female birds have ZW chromosomes, they were used for genomic DNA analysis. In all other experiments, male quail were used. The present study was approved by the Committee on Animal Experiments of the Graduate School of Bioagricultural Sciences, Nagoya University.

Microarray experiments. We used Affymetrix Chicken Genome Array. This array contains over 38,000 probe sets representing 32,773 transcripts. Genomic DNA individually extracted from liver using DNeasy tissue kit (QIAGEN) was labelled by BioPrime DNA labelling system (Invitrogen). The MBH was punched out (2.5 mm diameter) from 3 mm quail brain slices generated using a mouse brain matrix. Total RNA was prepared from two pools of three MBH at each time point to duplicate our observations on two arrays, using Trizol reagent (Invitrogen); cDNA synthesis and cRNA labelling reactions were performed with One-Cycle Target Labelling and Control Reagents Kit (Affymetrix). Hybridization, wash and stain protocols and scanning were performed using standard Affymetrix protocols. Data were analysed by using GeneSpring GX7.3 software (Agilent Technologies).

Full Methods and any associated references are available in the online version of the paper at www.nature.com/nature.

Received 22 July 2007; accepted 25 January 2008.

1. Dawson, A., King, V. M., Bentley, G. E. & Ball, G. F. Photoperiodic control of seasonality in birds. *J. Biol. Rhythms* **16**, 365–380 (2001).
2. Nicholls, T. J., Follett, B. K. & Robinson, J. E. A photoperiodic response in gonadectomised Japanese quail exposed to a single long day. *J. Endocrinol.* **97**, 121–126 (1983).
3. Follett, B. K., King, V. M. & Meddle, S. L. in *Biological Rhythms and Photoperiodism in Plants* (eds Lumsden, P. J. & Miller, A. J.) 231–242 (BIOS Scientific Publishers Ltd, Oxford, 1998).
4. Silver, R. *et al.* Coexpression of opsin- and VIP-like-immunoreactivity in CSF-contacting neurons of the avian brain. *Cell Tissue Res.* **253**, 189–198 (1988).
5. Yasuo, S., Watanabe, M., Okabayashi, N., Ebihara, S. & Yoshimura, T. Circadian clock genes and photoperiodism: comprehensive analysis of clock genes expression in the mediobasal hypothalamus, the suprachiasmatic nucleus and the pineal gland of Japanese quail under various light schedules. *Endocrinology* **144**, 3742–3748 (2003).
6. Sharp, P. J. & Follett, B. K. The effect of hypothalamic lesions on gonadotrophin release in Japanese quail (*Coturnix coturnix japonica*). *Neuroendocrinology* **5**, 205–218 (1969).
7. Juss, T. S. in *Avian Endocrinology* (ed. Sharp, P. J.) 47–60 (Society for Endocrinology, Bristol, UK, 1993).
8. Yoshimura, T. *et al.* Light-induced hormone conversion of T_4 to T_3 regulates photoperiodic response of gonads in birds. *Nature* **426**, 178–181 (2003).

9. Yasuo, S. *et al.* The reciprocal switching of two thyroid hormone-activating and -inactivating enzyme genes is involved in the photoperiodic gonadal response of Japanese quail. *Endocrinology* **146,** 2551–2554 (2005).
10. Follett, B. K. & Nicholls, T. J. Acute effect of thyroid hormones in mimicking photoperiodically induced release of gonadotropins in Japanese quail. *J. Comp. Physiol. B* **157,** 837–843 (1988).
11. Wada, M. Photoperiodic control of LH secretion in Japanese quail with special reference to the photoinducible phase. *Gen. Comp. Endocrinol.* **39,** 141–149 (1979).
12. Ueda, H. R. *et al.* A transcription factor response element for gene expression during circadian night. *Nature* **418,** 534–539 (2002).
13. Ganong, W. F. Circumventricular organs: definition and role in the regulation of endocrine and autonomic function. *Clin. Exp. Pharmacol. Physiol.* **27,** 422–427 (2000).
14. Grommen, S. V. H. *et al.* Molecular cloning, tissue distribution, and ontogenic thyroidal expression of the chicken thyrotropin receptor. *Endocrinology* **147,** 3943–3951 (2006).
15. Iwasawa, A. *et al.* Specific anti-peptide antibody to β subunit of chicken thyrotropin: production and characterization. *J. Reprod. Dev.* **48,** 197–204 (2002).
16. Turnbull, A. V. & Rivier, C. L. Intracerebroventricular passive immunization. II. Intracerebroventricular infusion of neuropeptide antisera can inhibit neuropeptide signalling in peripheral tissues. *Endocrinology* **139,** 128–136 (1998).
17. Maruyama, K. & Sugano, S. Oligo-capping: a simple method to replace the cap structure of eukaryotic mRNAs with oligoribonucleotides. *Gene* **138,** 171–174 (1994).
18. Murakami, M. *et al.* Expression and regulation of type II iodothyronine deiodinase in human thyroid gland. *Endocrinology* **142,** 2961–2967 (2001).
19. Panda, S. *et al.* Coordinated transcription of key pathways in the mouse by the circadian clock. *Cell* **109,** 307–320 (2002).
20. Rebay, I., Silver, S. J. & Tootle, T. L. New vision from Eyes absent: transcription factors as enzymes. *Trends Genet.* **21,** 163–171 (2005).
21. Matzuk, M. M., Kornmeier, C. M., Whitfield, G. K., Kourides, I. A. & Boime, I. The glycoprotein α-subunit is critical for secretion and stability of the human thyrotropin β-subunit. *Mol. Endocrinol.* **2,** 95–100 (1988).
22. Sharp, P. J. Tanycyte and vascular patterns in the basal hypothalamus of *Coturnix* quail with reference to their possible neuroendocrine significance. *Z. Zellforsch. Mikrosk. Anat.* **127,** 552–569 (1972).
23. Murakami, M. *et al.* Thyrotropin receptors in brown adipose tissue: thyrotropin stimulates type II iodothyroine deiodinase and uncoupling protein-1 in brown adipocytes. *Endocrinology* **142,** 1195–1201 (2001).
24. Takagi, T. *et al.* Involvement of transforming growth factor α in the photoperiodic regulation of reproduction in birds. *Endocrinology* **148,** 2788–2792 (2007).
25. Morgan, P. J. & Williams, L. M. The pars tuberalis of the pituitary: a gateway for neuroendocrine output. *Rev. Reprod.* **1,** 153–161 (1996).
26. Wittkowski, W., Bockmann, J., Kreutz, M. R. & Bockers, T. M. Cell and molecular biology of the pars tuberalis of the pituitary. *Int. Rev. Cytol.* **185,** 157–194 (1999).
27. Klosen, P. *et al.* The mt1 melatonin receptor and RORβ receptor are co-localized in specific TSH-immunoreactive cells in the pars tuberalis of the rat pituitary. *J. Histochem. Cytochem.* **50,** 1647–1657 (2002).
28. Juss, T., Meddle, S. M., Servant, R. S. & King, V. M. Melatonin and photoperiodic time measurement in the Japanese quail (*Coturnix coturnix japonica*). *Proc. R. Soc. Lond. B* **254,** 21–28 (1993).
29. Bockmann, J. *et al.* Thyrotropin expression in hypophyseal pars tuberalis-specific cells is 3,5,3′-triiodothyronine, thyrotropin-releasing hormone, and Pit-1 independent. *Endocrinology* **138,** 1019–1028 (1997).
30. Wittkowski, W., Bergmann, M., Hoffmann, K. & Pera, F. Photoperiod-dependent changes in TSH-like immunoreactivity of cells in the hypophysial pars tuberalis of the Djungarian hamster, *Phodopus sungorus*. *Cell Tissue Res.* **251,** 183–187 (1988).
31. Schaub, C., Bluet-Pajot, M. T., Szikla, G., Lornet, C. & Talairach, J. Distribution of growth hormone and thyroid-stimulating hormone in cerebrospinal fluid and pathological compartments in the central nervous system. *J. Neurol. Sci.* **31,** 123–131 (1977).
32. Hojvat, S., Baker, G., Kirsteins, L. & Lawrence, A. M. TSH in the rat and monkey brain: distribution, characterization and effect of hypophysectomy. *Neuroendocrinology* **34,** 327–332 (1982).
33. Bockmann, J., Winter, C., Wittkowski, W., Kreutz, M. R. & Bockers, T. M. Cloning and expression of a brain-derived TSH receptor. *Biochem. Biophys. Res. Commun.* **238,** 173–178 (1997).
34. Crisanti, P. *et al.* The expression of thyrotropin receptor in the brain. *Endocrinology* **142,** 812–822 (2001).
35. Lincoln, G. A., Clarke, I. J., Hut, R. A. & Hazlerigg, D. G. Characterizing a mammalian circannual pacemaker. *Science* **314,** 1941–1944 (2006).

Supplementary Information is linked to the online version of the paper at www.nature.com/nature.

Acknowledgements We thank T. Kondo and the Nagoya University Radioisotope Centre for use of facilities. We also thank J. A. Proudman and A. F. Parlow for providing the chicken luteinizing hormone radioimmunoassay kit and the bovine TSH, respectively. This work was done as a part of the Program for Promotion of Basic Research Activities for Innovative Biosciences (PROBRAIN) and, in part, by Grant-in-Aid for Scientific Research (S), (B), Grant-in-Aid for Young Scientists (S), Grant-in-Aid for JSPS Fellows from the Japanese Society for the Promotion of Science, and a grant of the Genome Network Project from the Ministry of Education, Culture, Sports, Science and Technology of Japan.

Author Contributions T.Yo. conceived and directed the work. N.N., H.O., T.Ya., T.A., T.T., K.H., S.Y., Y.K., S.K., Y.U. and T.Yo. performed the microarray analysis and *in situ* hybridization. N.N., T.K., H.R.U. and T.Yo. analysed the microarray data. N.N. performed the quantitative PCR and promoter assay. M.I. and P.J.S. determined the luteinizing hormone assay. H.O. and M.I. performed the ^{125}I-labelled TSH binding assay. T.Ya. and A.I. performed the immunocytochemistry. T.Ya., T.A. and A.I. examined the ICV injection and infusion. N.N., H.O., Y.S. and S.S. determined transcriptional start sites and genomic DNA sequences. T.Ni. cloned EYA, SIX and DACH family. M.M., T.Na. and S.E. provided laboratory facilities and new materials. All authors discussed the results and commented on the manuscript. T.Yo. and P.J.S. wrote the paper.

Author Information The microarray data and DNA sequence information have been deposited in NCBI Gene Expression Omnibus (GEO) (GSE8016–GSE8018) and DDBJ/EMBL/GenBank (AB307676–AB307681), respectively. Reprints and permissions information is available at www.nature.com/reprints. Correspondence and requests for materials should be addressed to T.Yo. (takashiy@agr.nagoya-u.ac.jp).

METHODS

Luteinizing hormone radioimmunoassay. Plasma luteinizing hormone concentrations of quail were determined by radioimmunoassay (RIA) as previously described[24,36].

Discrimination of long-day waves of gene expression. Pearson's correlation analysis was used to calculate the timing of the first and second waves of photoinduced gene expression. Correlation values were statistically tested and the peak time of the expression of each wave was determined by fitting a quadratic function to expression values of ±6 h around the time points with the maximum expression values.

***In situ* hybridization.** *In situ* hybridization was performed by using antisense and sense 45-nucleotide probes (Supplementary Table 4) as previously described[37]. No hybridization signal was observed in sense controls (data not shown).

Quantitative PCR. Reverse transcription was performed on total RNA (0.5 μg) using ReverTra Ace (Toyobo) and oligo-dT primers. Samples contained 1× SYBR Premix Ex Taq (Takara), 0.3 mM gene-specific primers (Supplementary Table 5) and 1/20 synthesized cDNA in a 25 μl volume. Quantitative PCR was performed in duplicates by using ABI Prism 7000 (Applied Biosystems) as follows: 95 °C for 10 s, then 40 cycles of 95 °C for 5 s, 60 °C for 30 s. We used *GAPDH* as an internal control.

Immunocytochemistry. Coronal frozen sections (20 μm) were fixed by 4% paraformaldehyde in 0.1 M phosphate buffer at pH 7.4 for 10 min at room temperature. Immunocytochemistry for the anti-chicken/quail TSH-β (1:5,000) was performed using Vectastain Elite ABC rabbit IgG kit (Vector Laboratories) with a standard protocol.

TSH binding assay. Bovine TSH (AFP8755, NIDDK) was labelled with ^{125}I by use of [^{125}I]Bolton-Hunter reagent (NEX120H, PerkinElmer) and purified by gel filtration using PD-10 column (GE Healthcare). Frozen sections were air-dried for 15 min, preincubated in the binding buffer (50 mM Tris-HCl buffer (pH 7.4) containing 0.1% BSA) at 37 °C for 1 h, and then incubated with ^{125}I-labelled TSH (78,000 c.p.m. per millilitre) in the binding buffer with (non-specific binding) or without (specific binding) cold bovine TSH (550 μg ml^{-1}, Sigma) at 37 °C for 1 h. Slides were rinsed in the ice-cold buffer without BSA (twice, 5 min each) followed by a rapid rinse in ice-cold distilled water to remove buffer salts. Labelled sections were apposed to BioMax MR (Kodak).

ICV TSH and TSH-β antibody administration. One week after the cannula implantation into the third ventricle of seven-week-old quail, we injected bovine TSH (T8931, Sigma) or TSH-β antibody through a guide cannula (24-gauge, 6 mm) and measured resulting changes in gene expression. We used bovine TSH, because avian TSH is unavailable and bovine TSH is known to activate avian TSHR[14]. An infrared viewer (NVR 2015, NEC) was used to facilitate TSH injection in darkness. An Alzet 2002 osmotic minipump was used for the prolonged ICV infusion of TSH, as previously reported[8].

Constructs. The 5′-flanking region of quail *DIO2* was subcloned into pGL3-basic vector (Promega) using 5′-ttgctgcctctcttctgccggatgaattca-3′ and 5′-tgaaagctctctcaatgcctcaaggtctg-3′. Deletion constructs and a mutated CRE site were created by PCR-based site-directed mutagenesis[38]. Mutation in the CRE site was generated by deletion of the central four nucleotides (−99: TGACGTCA → TGCA; −336: CCACGTCA → CCCA), as previously reported[39]. Quail *TSHR* cDNA was subcloned into pcDNA 3.1 vector (Invitrogen) using 5′-catgctgtggctgcctgtcgcct-3′, 5′-tcacagctcagtttgcctgc-3′. Constructs were verified by sequencing.

Transfection and luciferase assay. The 293 cells (RIKEN BRC Cell Bank) were plated in 24-well plates at a density of about 2×10^5 cells per well in 1 ml MEM supplemented with 10% fetal calf serum and 0.1 mM NEAA. *DIO2* promoter–luciferase construct (400 ng) was co-transfected with *TSHR* expression vector (400 ng) and the *Renilla* luciferase (phRL-TK, 2 ng, Promega) (for an internal control for transfection efficiency) using LipofectAMINE 2000 reagent (Invitrogen). After 24 h, cells were washed by PBS and treated with or without 1 mIU ml^{-1} bovine TSH (Sigma) in MEM medium. Five hours after this treatment, these media were washed with ice-cold PBS and transcriptional activity was determined using the dual-luciferase assay system (Promega) with Lumat LB950 (Berthold) according to the manufacturer's protocols. Firefly relative luciferase unit (RLU) measurements were normalized to *Renilla* RLU.

36. Krishnan, K. A., Proudman, J. A. & Bahr, J. M. Purification and partial characterization of isoforms of luteinizing hormone from the chicken pituitary gland. *Comp. Biochem. Physiol. B* **108**, 253–264 (2004).
37. Yoshimura, T. *et al.* Molecular analysis of avian circadian clock genes. *Brain Res. Mol. Brain Res.* **78**, 207–215 (2000).
38. Imai, Y., Matsushima, Y., Sugimura, T. & Terada, M. A simple and rapid method for generating a deletion by PCR. *Nucleic Acids Res.* **19**, 2785 (1991).
39. Travnickova-Bendova, Z., Cermakian, N., Reppert, S. M. & Sassone-Corsi, P. Bimodal regulation of mPeriod promoters by CREB-dependent signalling and CLOCK/BMAL1 activity. *Proc. Natl Acad. Sci. USA* **99**, 7728–7733 (2002).

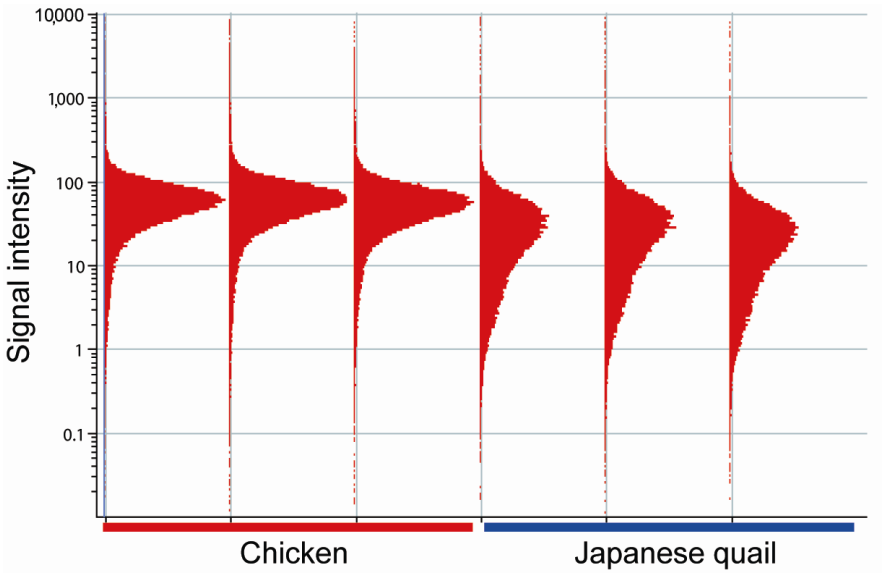

Supplementary Figure 1. Histogram showing hybridization signals for chicken (left) and quail (right) genomic DNA analyzed by Chicken GeneChip (n=3).

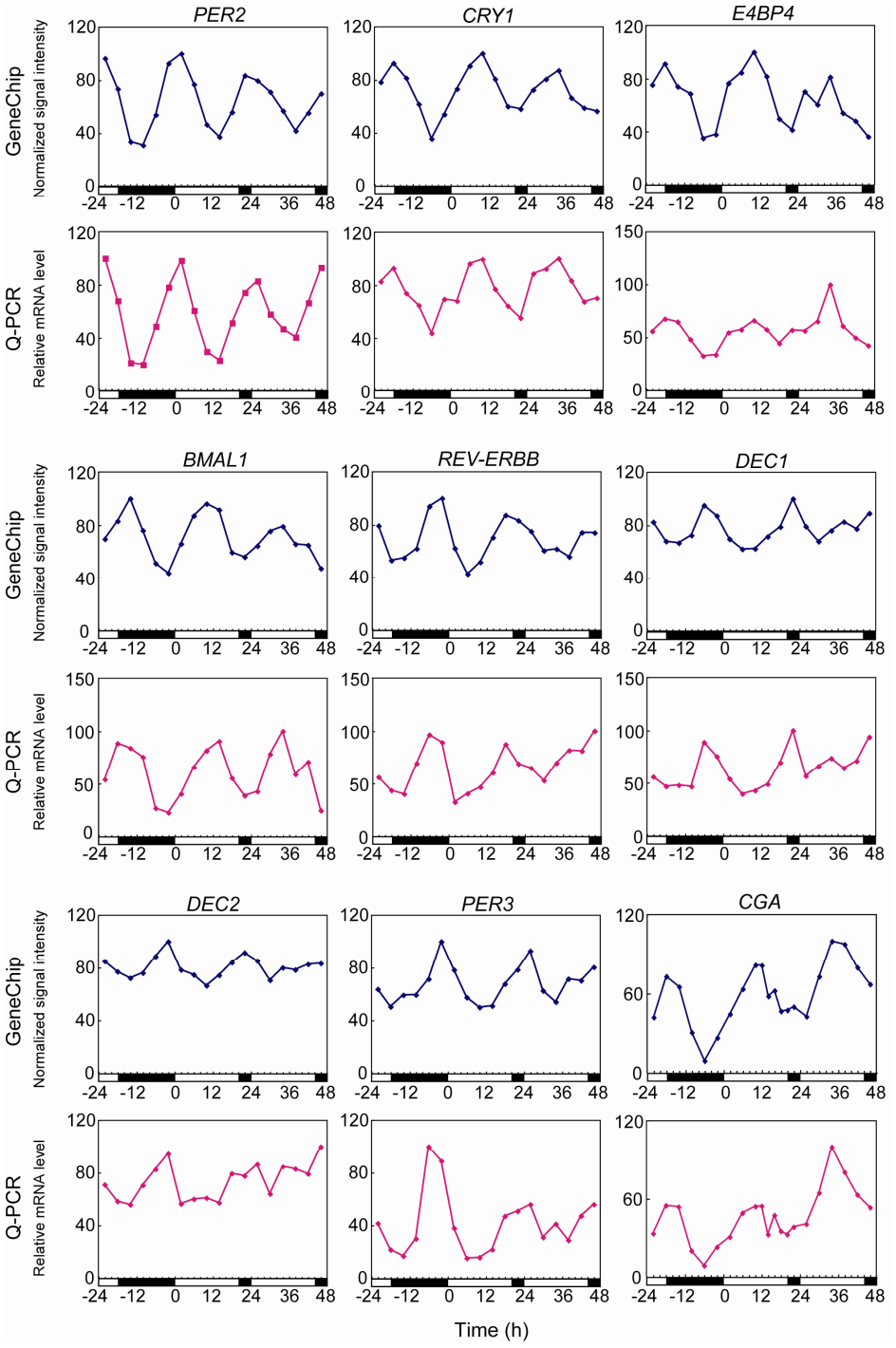

Supplementary Figure 2. Independent verification of microarray quantification. Relative mRNA levels of cycling clock genes and *CGA* (common pituitary glycoprotein alpha subunit) were measured with Q-PCR assay in the same samples that were used to prepare probes for microarray analysis. Quail *GAPDH* was used as the internal control.

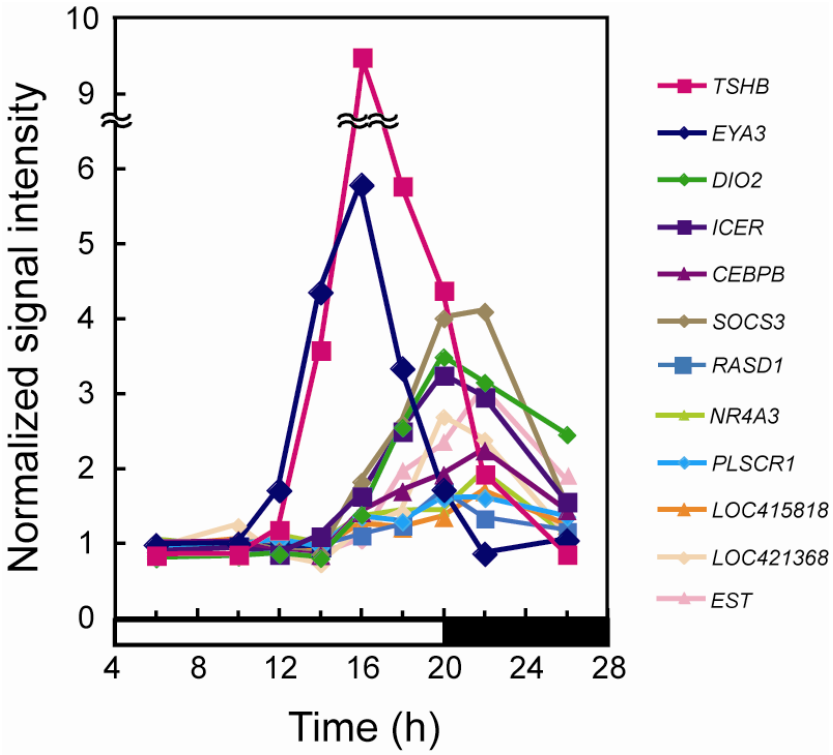

Supplementary Figure 3. Detailed temporal expression profile of 1st wave and 2nd wave genes during the photoinduction process determined by microarray. Data were normalized such that the median signal strength for each gene over all time points was 1.0. The average signal strength at each point was then displayed as a ratio relative to the median signal strength of that gene.

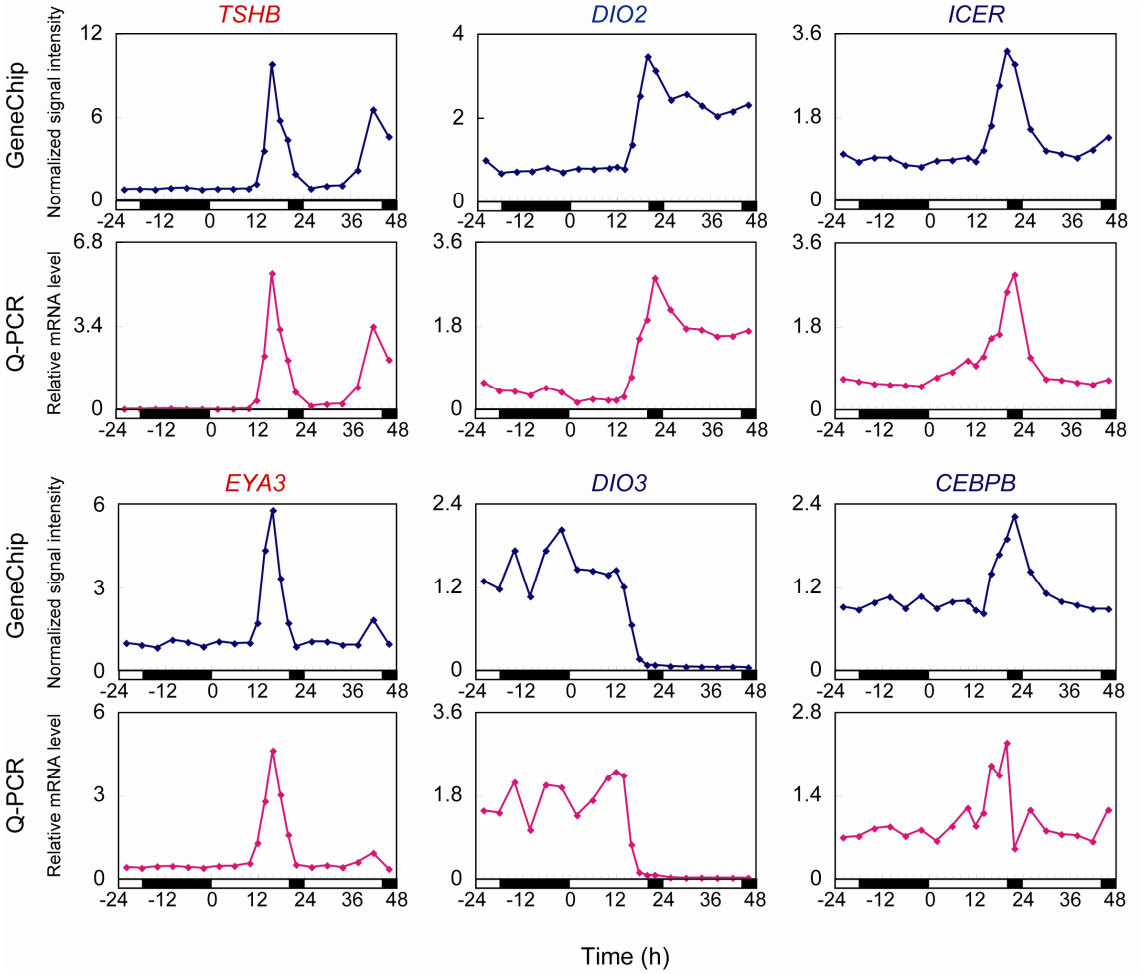

Supplementary Figure 4. Independent verification of microarray quantification. Relative mRNA levels of 1st wave (red characters) and 2nd wave genes (blue characters) were measured with Q-PCR assay in the same samples that were used to prepare probes for microarray analysis. Quail *GAPDH* was used as the internal control.

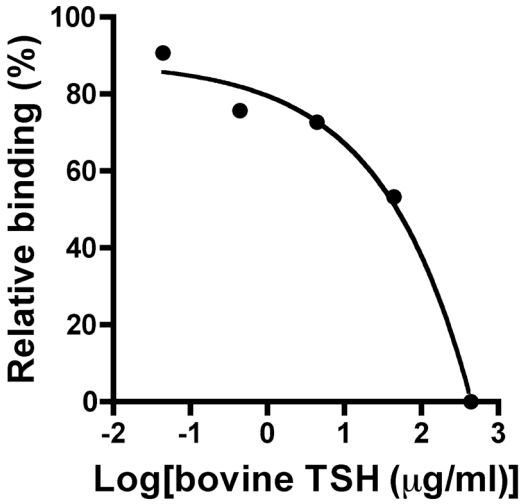

Supplementary Figure 5. Competitive inhibition by cold bovine TSH of ^{125}I-TSH binding to quail thyroid membranes. Specificity of ^{125}I-TSH binding was tested by radioreceptor assay (RRA) using quail thyroid membranes. Thyroid glands of quail were homogenized in ten volumes of ice-cold 50 mM Tris-HCl buffer (pH 7.4) with a teflon-glass homogenizer (3,000 rpm x 5 strokes). The homogenate was centrifuged at 40,000 g for 20 min at 4 ˚C. The pellet was washed, resuspended in the Tris-HCl buffer, and centrifuged for a second time under the same conditions. The crude membrane pellet was finally resuspended in Tris-HCl buffer (pH 7.5) and used for RRA. Binding was initiated by the addition of 100 μl aliquots of membranes to tubes containing ^{125}I-bovine TSH (Bolton-Hunter labelled, 17,500 cpm/50 μl in 50 mM Tris HCl (pH 7.4) containing 0.1 % BSA) in the presence of various concentrations of TSH (50 μl). After incubation at 37 ˚C for 1 h, tubes were centrifuged at 20,000 g for 2 min at 4 ˚C and the supernatants were aspirated. Then, the radioactivity of the pellet was counted with a γ-counter. Non-specific binding was defined as the binding in the presence of 550 μg/ml cold bovine TSH and the data was expressed as relative binding. Cold bovine TSH dose-dependently inhibited the binding of ^{125}I-TSH to the quail thyroid membranes.

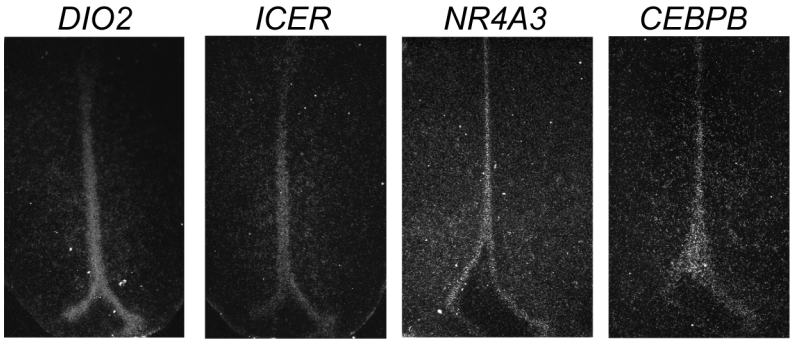

Supplementary Figure 6. Induction of four 2nd wave genes by ICV TSH injection was prominent in periventricular ependymal cells. Dark field photomicrographs of *in situ* hybridization are shown.

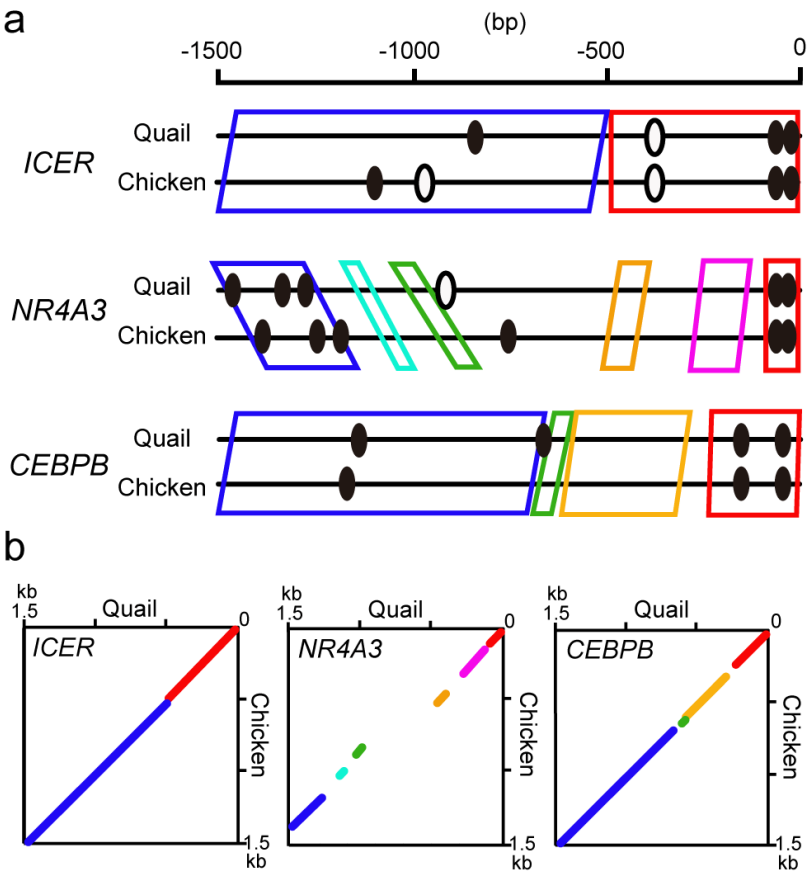

Supplementary Figure 7. Comparison of quail and chicken 2nd wave gene 5' upstream sequences. **a**. Conserved segments are boxed and putative CRE sites are shown as solid ovals. open oval: E and E'-boxes. **b**. Dot plot analysis of quail and chicken 5' upstream regions using BLASTN, with greater than 80% identity.

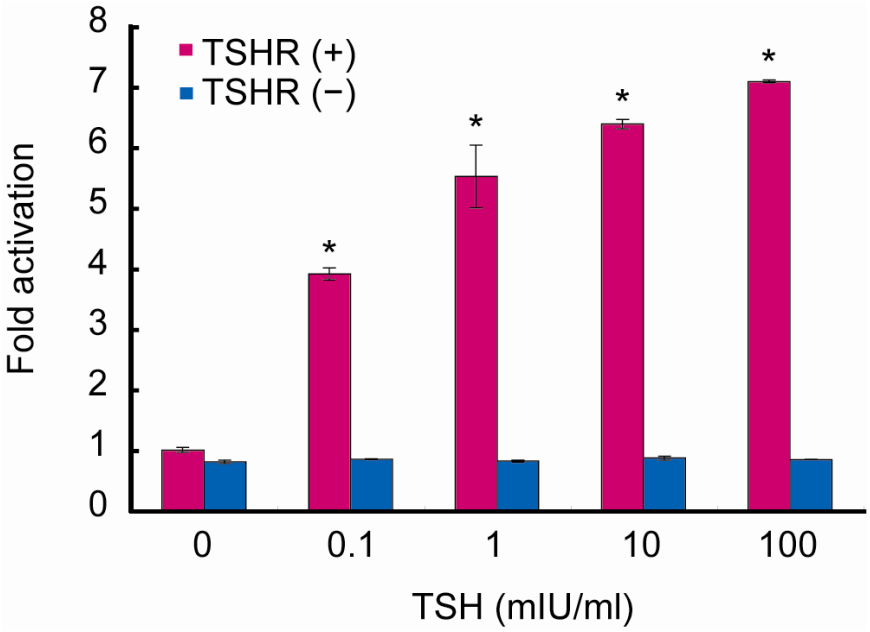

Supplementary Figure 8. Induction of *DIO2* mRNA by TSH requires TSHR. The transcriptional activation of a luciferase reporter containing a 1,642 bp fragment of the 5'-flanking region of the quail *DIO2* gene was assessed by co-transfection with quail *TSHR* expression vectors or empty vector in cultured 293 cells. Twenty four hours after transfection, the cells were incubated with bovine TSH (0, 0.1, 1, 10, 100 mIU/ml). The luciferase activity obtained from the reporter was normalized to the positive control *Renilla* luciferase reporter. Asterisks, P<0.01, *t*-test TSHR (+) versus TSHR (-).

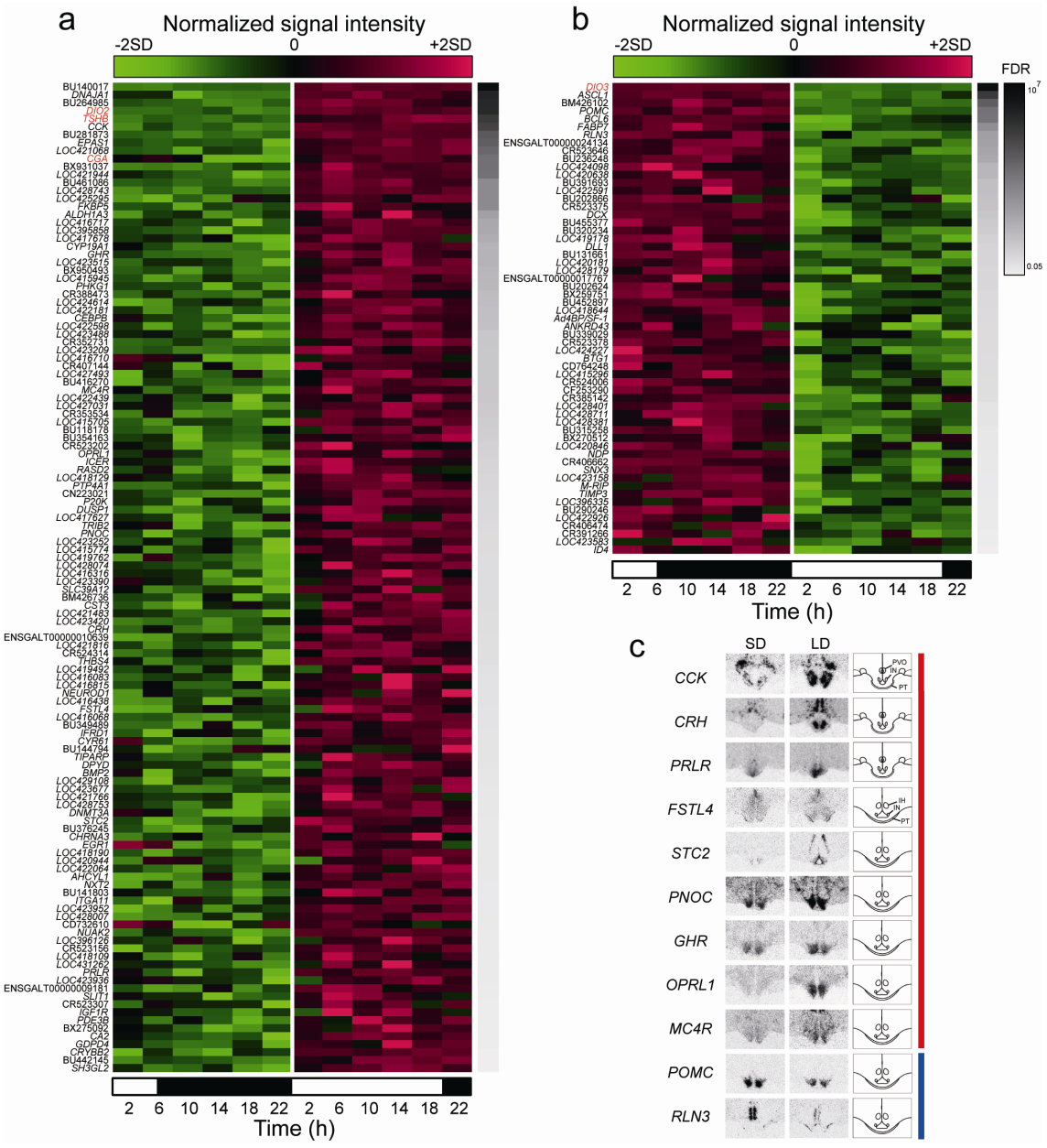

Supplementary Figure 9. Identification and localization in the MBH of differentially expressed genes over a 24 h period after chronic exposure to short or long day conditions (left and right hand sides of the panels respectively). Identification of 124 long day-up-regulated genes (**a**) and 59 down-regulated genes (**b**) and localization of expression of up-regulated (red bar) and down-regulated (blue bar) named genes (**c**).

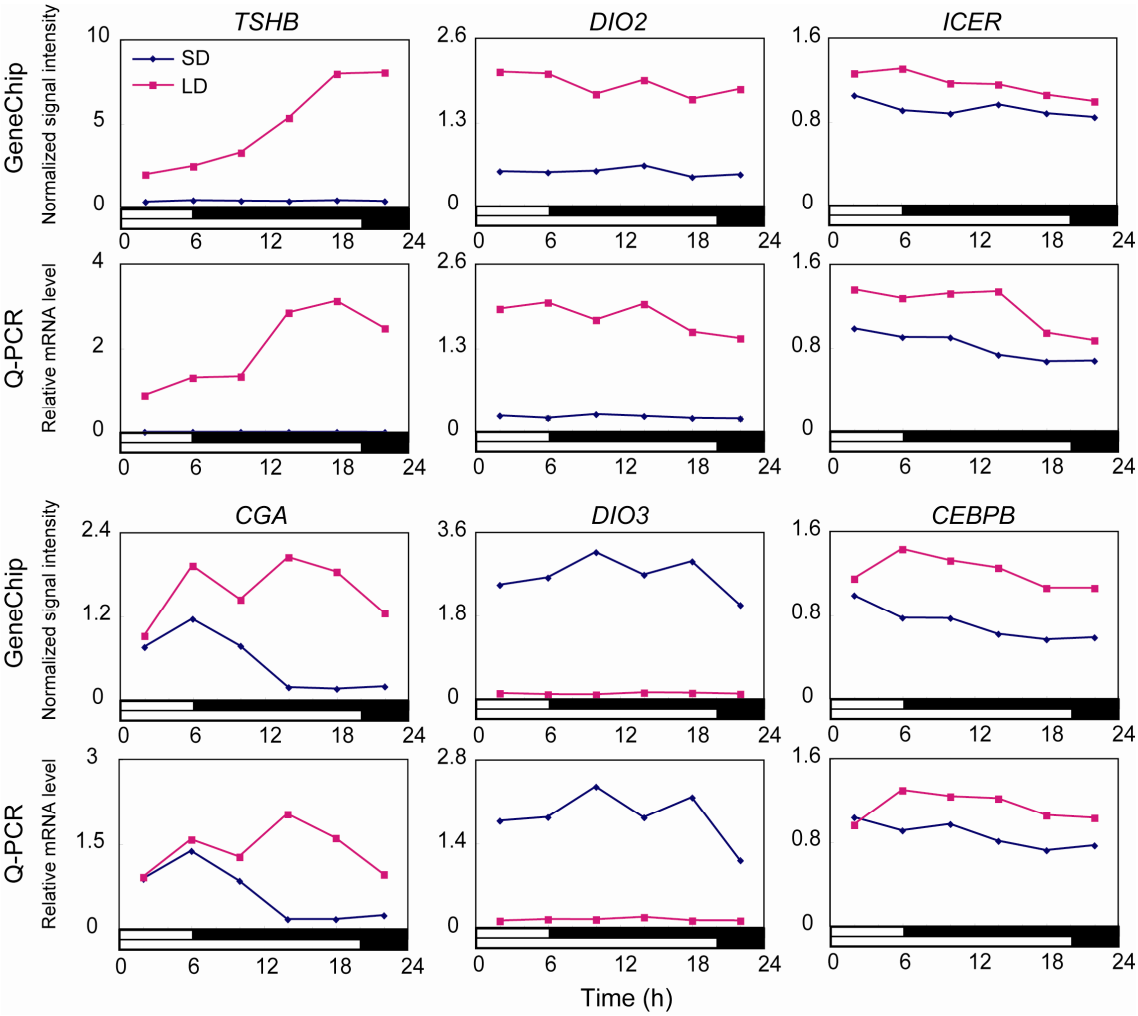

Supplementary Figure 10. Independent verification of microarray quantification. Relative mRNA levels of differentially expressed genes under short days (SD) and long days (LD) were measured with Q-PCR in the same samples that were used to prepare probes for GeneChip analysis. Quail *GAPDH* was used as the internal control.

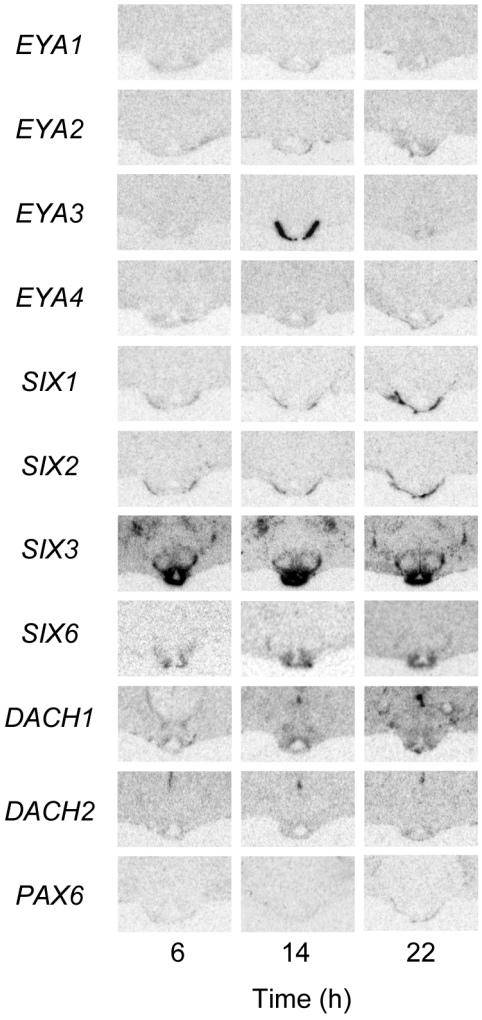

Supplementary Figure 11. Spatio-temporal expression profile of *EYA* (eyes absent), *SIX* (sine oculis), *DACH* (dachshund) family in the MBH of quail during the photoinduction process.

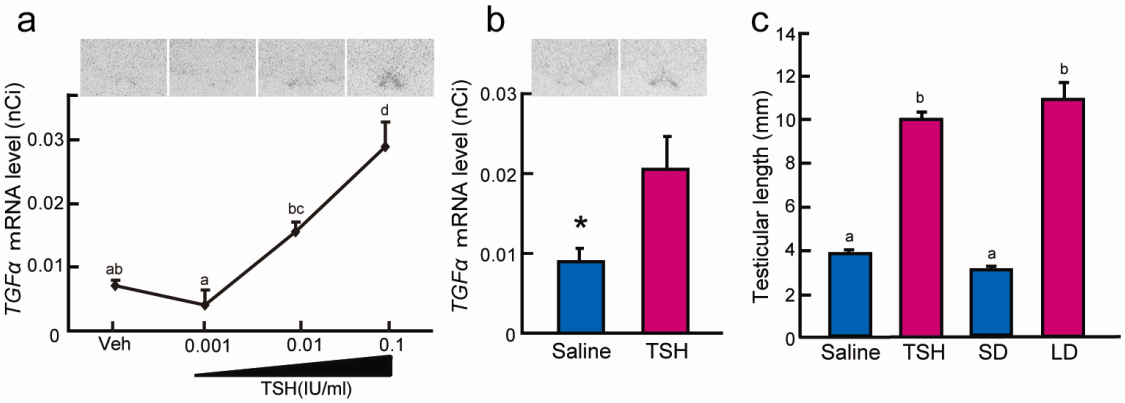

Supplementary Figure 12. Effect of TSH administration on *TGFα* mRNA and testicular growth. **a**. ICV injection of TSH induced *TGFα* expression in a dose dependent manner. Different characters indicate statistically significant differences (ANOVA, $F_{3,12}$=16.856, P<0.0001, Fisher's LSD post-hoc test P<0.05, n=3-5) **b,c**. Effect of chronic ICV infusion of TSH on MBH *TGFα* expression (**b**, *P<0.05, t-test, n=4,5) and testicular growth (**c**, Different characters indicate statistically significant differences. ANOVA, $F_{3,12}$=192.40, p<0.0001, Fisher's post-hoc test, p<0.001, n=3-5). SD: intact birds kept under short days; LD intact birds kept under long days for 2 weeks.

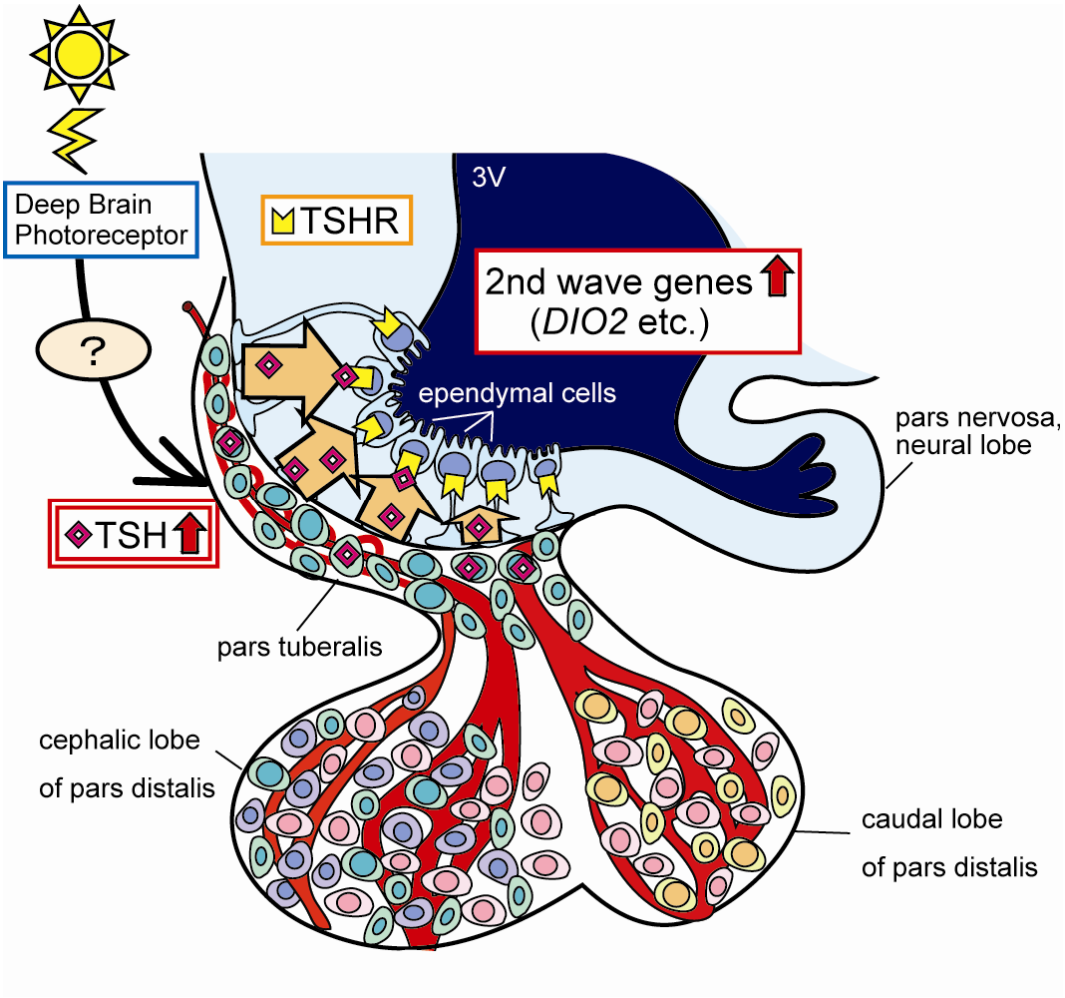

Supplementary Figure 13. Model of the mechanisms regulating photoperiodic time measurement in birds. Light information received by the deep brain photoreceptors induces expression of *TSHB* in the pars tuberalis (PT) of the pituitary gland. Long day-induced TSHβ and cycling CGA (common pituitary glycoprotein alpha subunit) form TSH in the PT and act on TSH receptor (TSHR) localized in ependymal cells lining the ventrolateral walls of third ventricle. Expression of 2nd wave genes includes *DIO2* is induced by TSH through TSHR-cAMP signalling pathway.

Supplementary Table 1

Supplementary table 1. Cycling genes in the MBH of the Japanese quail. Red characters indicates the circadian clock genes.

Affymetrix ID	Gene Symbol	Accession	Description	RefSeq	UniGene	Phase	P-value	FDR
Gga.1014.1.S1_at	PER2	CD732610	circadian clock protein		gga.1014	0.38	0	0
Gga.4107.1.S1_at	CRY1	NM_204245	cryptochrome 1 (photolyase-like)	NM_204245	gga.4107	6.57	1.28E-07	9.68E-04
GgaAffx.20805.1.S1_s_at	DLG5	CR523810	discs, large homolog 5 (Drosophila)	XM_421604	gga.20315	7.08	1.54E-05	2.47E-02
Gga.956.1.S1_at	NFIL3(E4BP4)	NM_204618	nuclear factor, interleukin 3 regulated	NM_204618	gga.956	7.14	2.23E-06	7.17E-03
Gga.17109.1.S1_at		CR388823	Finished cDNA, clone ChEST690b10		gga.17109	7.19	2.05E-07	1.03E-03
Gga.5710.1.S1_a_at	HTRA3	BX934040	HtrA serine peptidase 3	XM_420813	gga.5710	7.19	6.44E-05	4.86E-02
Gga.5520.1.S1_at		BX936168	Finished cDNA, clone ChEST146b12		gga.5520	7.44	8.19E-05	5.42E-02
GgaAffx.21135.1.S1_s_at	FGD3	CR523480	FYVE, RhoGEF and PH domain containing 3	XM_414331	gga.7018	7.51	1.12E-04	5.81E-02
Gga.15288.1.S1_at		CR385166	Finished cDNA, clone ChEST543o8		gga.15288	7.53	6.20E-05	4.86E-02
Gga.16071.1.S1_s_at	SGPL1	BU446083	sphingosine-1-phosphate lyase 1	NM_00100794	gga.16071	7.62	3.07E-05	3.32E-02
GgaAffx.3894.1.S1_s_at	LOC422242	ENSGALT00000010111	similar to Mtap7 protein	XM_420230		7.79	2.04E-05	2.81E-02
Gga.8797.1.S1_at		CD764248	Finished cDNA, clone ChEST189k11		gga.8797	7.83	5.60E-05	4.50E-02
GgaAffx.21243.1.S1_s_at	PHLPP; PLEKHE1	CR523372	PH domain and leucine rich repeat protein phosphatase	XM_418990	gga.20702	7.96	1.74E-04	7.78E-02
GgaAffx.10071.1.S1_at	CGA	ENSGALT00000025514	LOC421829	XM_429886		7.97	2.39E-05	3.07E-02
GgaAffx.21354.1.S1_at	LOC416774	CR523261	similar to Yippee-like protein 1 (DiGeorge syndrome-related protein FKSG3)	XM_415068		8.07	8.85E-05	5.50E-02
Gga.15971.1.S1_at		BU353686	Finished cDNA, clone ChEST136j22		gga.15971	8.08	1.07E-04	5.77E-02
Gga.7044.3.S1_s_at	SEPP1	BU244903	selenoprotein P, plasma, 1	NM_00103160	gga.7044	8.23	3.06E-06	8.42E-03
Gga.7016.1.S1_at	PAPSS1	BU138060	3'-phosphoadenosine 5'-phosphosulfate synthase 1	XM_420493	gga.10727	8.31	2.21E-04	8.43E-02
Gga.1329.1.S1_at	ARNTL; BMAL1	AF246957	aryl hydrocarbon receptor nuclear translocator-like	NM_00100146	gga.1329	8.52	1.51E-07	9.68E-04
Gga.16254.1.S1_at		CR386060	Finished cDNA, clone ChEST237h3		gga.16254	8.64	2.11E-04	8.39E-02
GgaAffx.22378.1.S1_s_at	LOC425395	ENSGALT00000012718	similar to 1-phosphatidylinositol-4,5-bisphosphate phosphodiesterase gamma 2 (Phosphoinositide phospholipase C) (PLC-gamma-2) (Phospholipase C-gamma-2) (PLC-IV)	XM_423160		8.73	9.61E-05	5.70E-02
Gga.3477.1.S1_at	FGFR2; BEK; cek3	NM_205319	fibroblast growth factor receptor 2 (bacteria-expressed kinase, keratinocyte growth factor receptor, craniofacial dysostosis 1, Crouzon syndrome, Pfeiffer syndrome, Jackson-Weiss syndrome)	NM_205319	gga.3477	8.82	9.90E-08	9.54E-04
GgaAffx.12938.9.S1_at	TARDBP	AJ719699	TAR DNA binding protein	NM_00103087	gga.16753	8.84	7.37E-05	5.17E-02
GgaAffx.22381.3.S1_at	NCAM1	ENSGALT00000012725	neural cell adhesion molecule 1	XM_425812		8.84	3.53E-05	3.58E-02
Gga.6073.1.S1_at		BU415550	Finished cDNA, clone ChEST152d3		gga.6073	9.02	1.43E-05	2.47E-02
GgaAffx.2851.1.S1_at	LOC424441	ENSGALT00000007329	similar to heme binding protein 2; putative heme-binding protein	XM_422283		9.10	2.32E-04	8.67E-02
Gga.3242.1.S1_at	LOC419338	AL587491	similar to novel amplified in breast cancer-1	XM_417504		9.35	1.38E-04	6.81E-02
Gga.2875.1.S1_at	ACVR1	NM_204560	activin A receptor, type I	NM_204560	gga.2875	9.40	1.06E-04	5.77E-02
Gga.1609.1.S1_at	APOH	BX932102	apolipoprotein H (beta-2-glycoprotein I)	XM_415683	gga.1609	9.64	9.77E-05	5.70E-02
GgaAffx.7899.1.S1_at	LOC424308	ENSGALT00000020351	similar to KIAA1461 protein	XM_422153		9.65	9.08E-05	5.56E-02
Gga.1999.1.S1_a_at	CRYAB	U26661	crystallin, alpha B	NM_205176	gga.1999	9.67	9.37E-05	5.64E-02
Gga.16213.1.S1_at		CR387761	Finished cDNA, clone ChEST532c9		gga.16213	9.72	2.36E-04	8.76E-02
GgaAffx.25359.2.A1_at		ENSGALT00000003108				9.72	2.55E-04	9.10E-02
GgaAffx.25365.1.S1_at	COMT	ENSGALT00000003148	catechol-O-methyltransferase	XM_415077	gga.7199	9.83	2.97E-04	9.95E-02
GgaAffx.20301.1.S1_at		CR524314	Finished cDNA, clone ChEST819a3		gga.20550	9.85	1.86E-05	2.65E-02
Gga.17320.1.S1_at		CR388514	Finished cDNA, clone ChEST1018l10		gga.17320	9.93	8.31E-05	5.42E-02

Supplementary Table 1

Affymetrix ID	Gene Symbol	Accession	Description	RefSeq	UniGene	Phase	P-value	FDR
Gga.4058.1.S1_at	LOC396473	NM_205480	myristoylated alanine-rich C kinase substrate (MARCKS)	NM_205480	gga.4058	10.14	1.97E-04	8.34E-02
GgaAffx.8704.1.S1_at		ENSGALT00000022222				10.18	6.51E-06	1.39E-02
Gga.1026.2.S1_a_at	LOC427675	BU104660	similar to Rps15a protein	XM_425249		10.52	1.45E-04	6.95E-02
GgaAffx.20516.1.S1_s_at		CR524099	Finished cDNA, clone ChEST262g11		gga.13061	10.69	2.78E-05	3.32E-02
Gga.5178.1.S1_at	LOC424570	BU485658	similar to receptor protein tyrosine phosphatase LAR	XM_422409		10.95	4.35E-05	3.81E-02
GgaAffx.2789.1.S1_at	LOC416371	ENSGALT00000007194	similar to betaine homocysteine methyl transferase	XM_414685		11.14	8.91E-07	3.43E-03
GgaAffx.12959.1.S1_at	IPO13	AJ720856	importin 13	NM_00100653	gga.22612	11.24	3.95E-05	3.80E-02
GgaAffx.12308.1.S1_s_at	PKP4	AJ720205	plakophilin 4	NM_00100652	gga.5277	11.38	3.09E-05	3.32E-02
GgaAffx.4781.1.S1_at	LOC425380	ENSGALT00000012398	similar to protein kinase C-theta	XM_423148		11.90	8.44E-05	5.42E-02
GgaAffx.24104.1.S1_at	LOC418178	ENSGALT00000021384	similar to glutathione S-transferase	XM_416409		12.12	1.62E-04	7.61E-02
GgaAffx.3833.5.S1_at	SCN5A; LOC430306	ENSGALT00000009919	oltage-gated sodium channel type V alpha	XM_418535 ; XM_427864	gga.564	12.43	2.66E-04	9.25E-02
Gga.2154.1.S1_at		BU379404	Finished cDNA, clone ChEST794n20		gga.2154	13.05	3.78E-05	3.73E-02
Gga.1527.1.S1_at	LOC426871	BX931252	similar to DKFZP586A0522 protein	XM_424479	gga.1527	14.33	4.75E-06	1.22E-02
Gga.1308.2.S1_at	KIF20A	CR388986	Kinesin family member 20A	NM_00101278	gga.1308	18.38	2.14E-04	8.39E-02
Gga.4315.1.S2_at	NR1D2; REV-ERBB	BU434806	nuclear receptor subfamily 1, group D, member 2	NM_205205	gga.4315	19.47	2.14E-07	1.03E-03
Gga.15700.1.S1_at	bHLHB2(DEC1)	BU144794	Finished cDNA, clone ChEST258o16		gga.15700	19.65	5.91E-06	1.37E-02
Gga.10816.1.S1_at		BX932362	Finished cDNA, clone ChEST355i12		gga.10816	20.04	1.70E-04	7.78E-02
Gga.10636.1.S1_at		BX932098	Finished cDNA, clone ChEST38a21		gga.10636	20.07	2.17E-04	8.39E-02
GgaAffx.6473.1.A1_at		ENSGALT00000016696				20.31	1.07E-04	5.77E-02
Gga.14127.1.S1_at		BU118866	Finished cDNA, clone ChEST140e9		gga.14127	20.39	4.68E-05	4.01E-02
Gga.9491.1.S1_at	LOC417217	BU228626	similar to Dynamin-1	XM_415501		20.62	7.56E-06	1.53E-02
Gga.1229.1.S1_at	bHLHB3(DEC2)	BU244306	Finished cDNA, clone ChEST132b22		gga.1229	20.64	1.37E-06	4.80E-03
GgaAffx.21040.1.S1_s_at		CR523575	Finished cDNA, clone ChEST537j12		gga.9927	20.73	1.21E-04	6.21E-02
GgaAffx.22193.1.S1_s_at	CADPS	ENSGALT00000011770	Ca2+-dependent secretion activator	XM_414412	gga.16126	20.83	4.17E-05	3.80E-02
Gga.8026.1.S1_at		BX275469	Transcribed locus		gga.8026	20.91	2.91E-04	9.83E-02
Gga.11.1.S1_at	HCRT	NM_204185	hypocretin (orexin) neuropeptide precursor	NM_204185	gga.11	21.00	2.66E-04	9.20E-02
Gga.10186.1.S1_at	IGSF4D	BX950409	immunoglobulin superfamily, member 4D	XM_416672	gga.10186	21.05	6.81E-05	4.86E-02
Gga.203.1.S1_at	SNCB	NM_204671	synuclein, beta	NM_204671	gga.203	21.11	3.11E-05	3.32E-02
Gga.10505.1.S1_at		BU477621	Finished cDNA, clone ChEST53b5		gga.10505	21.17	2.40E-04	8.79E-02
GgaAffx.11545.1.S1_s_at	MDH1	AJ719442	malate dehydrogenase 1, NAD (soluble)	NM_00100639	gga.1141	21.20	1.84E-04	8.05E-02
Gga.2726.1.S1_at	SNCA	NM_204673	synuclein, alpha (non A4 component of amyloid	NM_204673	gga.2726	21.21	9.91E-05	5.70E-02
Gga.4730.1.S1_at		CR387467	Finished cDNA, clone ChEST490o21		gga.4730	21.21	1.06E-05	2.05E-02
Gga.17835.1.S1_at		BU312867	Finished cDNA, clone ChEST198e11		gga.17835	21.30	2.49E-04	8.96E-02
GgaAffx.349.4.S1_s_at	PER3	ENSGALT00000000799	circadian clock protein	XM_417527		21.54	1.52E-05	2.47E-02
Gga.1673.1.A1_at		AL588323	Finished cDNA, clone ChEST883o18		gga.1673	22.07	2.48E-04	8.96E-02
Gga.5353.1.S1_at		BU354163	Transcribed locus, weakly similar to XP_425603.1 PREDICTED: similar to ORF2 [Gallus gallus]		gga.5353	22.20	2.16E-04	8.39E-02
Gga.5129.1.S1_at	ALC	NM_204440	ALC protein	NM_204440	gga.5129	22.38	1.75E-04	7.78E-02
Gga.14806.1.S1_at		BX273662	Finished cDNA, clone ChEST39h14		gga.14806	22.50	1.82E-05	2.65E-02
Gga.4148.1.S1_at	TPI1	NM_205451	triosephosphate isomerase 1	NM_205451	gga.4148	22.81	2.73E-04	9.38E-02
GgaAffx.9414.1.S1_at	LOC421058	ENSGALT00000023921	similar to elastin microfibril interfacer 2; extracellular glycoprotein EMILIN-2 precursor	XM_419145		23.18	6.31E-05	4.86E-02
GgaAffx.12473.1.S1_s_at	ZA20D2	AJ720370	zinc finger, A20 domain containing 2	NM_00103142	gga.11716	23.29	1.78E-05	2.65E-02

Supplementary Table 2. Photoperiodically induced genes during the photoinduction process in the MBH of the Japanese quail.
Red characters and blue characters indicate 1st wave and 2nd wave genes, respectively.

Affymetrix ID	Gene Symbol	Accession	Description	RefSeq	UniGene
Gga.551.1.S1_at	TSHB; TSH-B	NM_205063	thyroid stimulating hormone, beta	NM_205063	gga.551
GgaAffx.508.1.S1_at	EYA3	ENSGALT00000001127	Eya3 protein	XM_417715	gga.1018
Gga.1819.1.S1_at	DIO2	NM_204114	deiodinase, iodothyronine, type II	NM_204114	gga.1819
Gga.6220.1.S1_a_at	ICER	NM_204387	ICER protein	NM_204387	gga.6220
Gga.4285.1.S1_at	CEBPB; NF-M	NM_205253	CCAAT/enhancer binding protein (C/EBP), beta	NM_205253	gga.4285
Gga.13328.1.S1_at	NR4A3	BU436288	nuclear receptor subfamily 4 group A member 3	XM_419081	gga.33742
Gga.915.1.S1_at	SOCS3	NM_204600	suppressor of cytokine signaling 3	NM_204600	gga.915
GgaAffx.12426.1.S1_s_at	PLSCR1	AJ720323	phospholipid scramblase 1	XM_422696	gga.7604
Gga.9972.1.S1_at	RASD1	BX930456	RAS, dexamethasone-induced 1	XM_414811	gga.9972
GgaAffx.3568.1.S1_at	LOC415818	ENSGALT00000009128	similar to hypothetical protein DKFZp434B044	XM_414180	
Gga.2461.1.S1_at		BU264985	Transcribed locus		gga.2461
Gga.10787.1.S1_at	LOC421368	BX932508	similar to Jun dimerization protein p21SNFT	XM_419428	gga.10787
Gga.552.1.S1_at	DIO3	Y11273	deiodinase, iodothyronine, type III	XM_426465	gga.552

Supplementary Table 3

Supplementary Table 3. Differentially expressed genes between short and long day conditions. Black and blue characters indicate long day-up-regulated genes and -down-regulated genes, respectively.

Affymetrix ID	P-value	Gene Symbol	Accession	Description	RefSeq	UniGene
Gga.17403.1.S1_at	1.50E-07		BU140017	Finished cDNA, clone ChEST724o21		gga.17403
Gga.552.1.S1_at	1.63E-07	DIO3	Y11273	deiodinase, iodothyronine, type III	XM_426465	gga.552
Gga.5644.1.S1_s_at	7.69E-07	DNAJA1	BX271179	DnaJ (Hsp40) homolog, subfamily A, member 1	NM_001012945	gga.5644
Gga.2461.1.S1_at	9.58E-07		BU264985	Transcribed locus		gga.2461
Gga.1819.1.S1_at	1.03E-06	DIO2	NM_204114	deiodinase, iodothyronine, type II	NM_204114	gga.1819
Gga.551.1.S1_at	2.69E-06	TSHB; TSH-B	NM_205063	thyroid stimulating hormone, beta	NM_205063	gga.551
Gga.488.1.S1_at	2.76E-06	ASCL1	NM_204412	achaete-scute complex-like 1(Drosophila)	NM_204412	gga.488
GgaAffx.21834.1.S1_s_at	4.22E-06	CCK	NM_001001741	cholecystokinin	NM_001001741	gga.2441
Gga.9368.1.S1_at	1.45E-05		BU281873			
Gga.3035.1.S1_at	1.84E-05	EPAS1	NM_204807	endothelial PAS domain protein 1	NM_204807	gga.3035
Gga.19300.1.S1_at	1.84E-05		BM426102	Finished cDNA, clone ChEST556c20		gga.19300
GgaAffx.9485.1.S1_at	2.81E-05	LOC421068	ENSGALT00000024095	similar to lung alpha/beta hydrolase fold protein 3	XM_419156	
GgaAffx.10071.1.S1_at	4.65E-05	LOC421829(CGA)	ENSGALT00000025514	LOC421829	XM_429886	
Gga.7364.1.S1_a_at	4.65E-05		BX931037	Finished cDNA, clone ChEST446b11		gga.7364
GgaAffx.24962.1.S1_s_at	4.77E-05	LOC421944	ENSGALT00000026546	similar to GREB1 protein isoform a; gene regulated by estrogen in breast cancer protein	XM_419956	
Gga.6271.1.S1_at	5.11E-05	POMC	BX540524	proopiomelanocortin (adrenocorticotropin/ beta-lipotropin/ alpha-melanocyte stimulating hormone/ beta-melanocyte stimulating hormone/ beta-endorphin)	NM_001031098	gga.6271
GgaAffx.11648.1.S1_at	5.63E-05	BCL6	AJ719545	B-cell CLL/lymphoma 6 (zinc finger protein 51)	NM_001012930	gga.4457
Gga.12627.1.S1_at	0.000184		BU461086			
GgaAffx.23246.2.S1_s_at	0.000184	LOC428743	ENSGALT00000017135	similar to alanine-glyoxylate aminotransferase 2-like 1	XM_426301	
GgaAffx.3940.1.S1_at	0.000184	LOC425295	ENSGALT00000010212	similar to Chloride channel protein 2 (ClC-2)	XM_423073	
GgaAffx.22637.1.S1_s_at	0.000184	FKBP5; FKBP51; PPIase	ENSGALT00000001399	FK506 binding protein 5	NM_001005431	gga.4750
Gga.4318.1.S1_at	0.00025	FABP7	NM_205308	fatty acid binding protein 7, brain	NM_205308	gga.4318
Gga.12454.1.S1_at	0.000628	LOC427223; RLN3	BU435007	similar to relaxin 3 preproprotein; insulin-like 7	XM_424810	
Gga.3807.1.S2_s_at	0.000706	ALDH1A3; ALDH6	NM_204669	aldehyde dehydrogenase 1 family, member A3	NM_204669	gga.3807
GgaAffx.24555.1.S1_s_at	0.000778		ENSGALT00000024134	Finished cDNA, clone ChEST284i20		gga.4865
GgaAffx.20969.1.S1_at	0.000954		CR523646	Finished cDNA, clone ChEST322a24		gga.20399
Gga.12773.1.S1_at	0.00107	LOC416717	BX950498	similar to chromosome 20 open reading frame 39	XM_415014	gga.12773
Gga.3138.1.S1_a_at	0.00108	LOC395858	NM_205007	histone macroH2A1.2	NM_205007	gga.3138
Gga.16384.1.S1_at	0.00109		BU236248	Finished cDNA, clone ChEST229g1		gga.16384
GgaAffx.26692.1.S1_at	0.00144	LOC417678	ENSGALT00000009642	similar to solute carrier family 13 (sodium-dependent citrate transporter), member 5; sodium-coupled citrate transporter	XM_415923	
GgaAffx.21816.1.S1_s_at	0.00201	CYP19A1	NM_001001761	cytochrome P450, family 19, subfamily A, polypeptide 1	NM_001001761	gga.859
Gga.9233.1.S1_at	0.00203	GHR	BU231940	Growth hormone receptor precursor		gga.9233
GgaAffx.23689.1.S1_at	0.00203	LOC423515	ENSGALT00000019348	LOC423515	XM_430062	
Gga.18427.1.S1_at	0.00246	LOC424098	BU213226	hypothetical gene supported by CR390562	XM_430126	gga.18427
Gga.12774.1.S1_at	0.00252		BX950493	Finished cDNA, clone ChEST523o19		gga.12774
GgaAffx.7118.1.S1_s_at	0.00252	LOC420638	ENSGALT00000018264	similar to 2-hydroxyphytanoyl-CoA lyase (2-HPCL)	XM_418737	
GgaAffx.26220.2.S1_s_at	0.00264	LOC415945	ENSGALT00000007128	similar to semaphorin sem2	XM_414289	
Gga.6022.1.S1_s_at	0.00278	PHKG1	BU106819	phosphorylase kinase, gamma 1 (muscle)	NM_001006217	gga.6022

Supplementary Table 3

Affymetrix ID	P-value	Gene Symbol	Accession	Description	RefSeq	UniGene
Gga.17706.1.S1_at	0.00331		CR388473	Finished cDNA, clone ChEST591g11		gga.17706
Gga.7143.2.S1_a_at	0.00354	LOC424614	BU386059	similar to fatty acid amide hydrolase	XM_422450	
Gga.18324.1.S1_s_at	0.00386		BU391693	Finished cDNA, clone ChEST228a16		gga.18324
GgaAffx.23445.1.S1_s_at	0.0041	LOC422591	ENSGALT00000018050	similar to protein tyrosine phosphatase, non-receptor type 13 isoform 2; protein tyrosine phosphatase, nonreceptor type 13; protein-tyrosine phosphatase PTPL1; protein tyrosine phosphatase 1E; Fas-associated phosphatase-1	XM_420550	
GgaAffx.2984.1.S1_s_at	0.00414	LOC422181	ENSGALT00000007661	similar to Phosphorylase B kinase alpha regulatory chain, skeletal muscle isoform (Phosphorylase kinase alpha M	XM_420177	
Gga.4285.1.S1_at	0.00414	CEBPB; NF-M	NM_205253	CCAAT/enhancer binding protein (C/EBP), beta	NM_205253	gga.4285
Gga.6052.3.S1_a_at	0.00431	LOC422598	BU300073	similar to acyl-CoA-desaturase	XM_420557	
Gga.14762.1.S1_at	0.00455		BU202866	Finished cDNA, clone ChEST103n10		gga.14762
GgaAffx.21240.1.S1_at	0.00466		CR523375	Finished cDNA, clone ChEST853e7		gga.16698
Gga.2608.1.S1_at	0.00548	DCX; 18C15.5	NM_205204	doublecortex; lissencephaly, X-linked (doublecortin)	NM_204335	gga.2608
GgaAffx.7332.1.S1_at	0.00558	LOC423488	ENSGALT00000018877	similar to hypothetical protein	XM_421393	
Gga.14263.1.S1_at	0.00558		CR352731	Finished cDNA, clone ChEST39a12		gga.14263
Gga.4003.1.S1_at	0.00593	LOC423209	BU143709	similar to hypothetical protein MGC4504	XM_421133	gga.4003
Gga.16760.1.S1_at	0.006	LOC416710	BU326734	similar to RNA polymerase I polypeptide B; DNA-directed RNA polymerase I 135kDa polypeptide; RNA polymerase I	XM_415007	
Gga.19895.1.S1_at	0.006		CR407144	Finished cDNA, clone ChEST749n19		gga.19895
Gga.11081.1.S1_s_at	0.006	LOC427493	CF255496	similar to RANTES factor of late activated T lymphocytes-1	XM_425065	
Gga.9734.1.S1_at	0.006		BU416270	Finished cDNA, clone ChEST612l15		gga.9734
GgaAffx.8162.1.S1_at	0.00613	MC4R	ENSGALT00000021044	melanocortin 4 receptor	NM_001031514	gga.32096
Gga.11300.1.S1_at	0.0063	LOC422439	BU348384	similar to E74-like factor 2 (ets domain transcription factor) isoform 2; new Ets-related factor	XM_420406	
GgaAffx.1176.1.S1_at	0.00696	LOC427031	ENSGALT00000002758	similar to HECT domain containing 2	XM_424632	
Gga.13008.1.S1_at	0.00732		CR353534	Finished cDNA, clone ChEST11k17		gga.13008
Gga.16449.1.S1_at	0.00734		BU455377	Finished cDNA, clone ChEST1038b12		gga.16449
GgaAffx.2068.1.S1_at	0.00795	LOC415705	ENSGALT00000005243	similar to neuronal calcium binding protein 2	XM_414072	
Gga.2606.1.S1_at	0.00808		BU320234	Finished cDNA, clone ChEST380k16		gga.2606
Gga.5461.1.S1_at	0.00865		BU118178	Finished cDNA, clone ChEST938n22		gga.5461
Gga.5353.1.S1_at	0.00926		BU354163	Transcribed locus, weakly similar to XP_425603.1 PREDICTED: similar to ORF2 [Gallus gallus]		gga.5353
Gga.11231.1.S1_at	0.01	LOC419178	BX929984	similar to growth hormone-releasing hormone/pituitary adenylate cyclase-activating polypeptide precursor	XM_417357	gga.11231
GgaAffx.21413.1.S1_s_at	0.0108		CR523202	Finished cDNA, clone ChEST629c13		gga.17584
GgaAffx.9726.1.S1_at	0.0113	LOC428533, OPRL1	ENSGALT00000024646	similar to opioid receptor, kappa 1; Opiate receptor, kappa-1	XM_426087	
Gga.2283.1.S2_at	0.0125	DLL1	BU227707	delta-like 1 (Drosophila)	NM_204973	gga.2283
Gga.15955.1.S1_s_at	0.0126		BU131661	Finished cDNA, clone ChEST147b19		gga.1750
Gga.6220.2.S1_a_at	0.0127	ICER	BX931695	ICER protein	NM_204387	gga.6220
Gga.11996.1.S1_at	0.0127	RASD2	BX933905	RASD family, member 2	XM_416293	gga.11996
GgaAffx.24735.1.S1_at	0.0133	LOC420181	ENSGALT00000025208	LOC420181	XM_429743	

Supplementary Table 3

Affymetrix ID	P-value	Gene Symbol	Accession	Description	RefSeq	UniGene
GgaAffx.751.1.S1_s_at	0.0145	LOC428179	ENSGALT00000001684	similar to membrane metallo-endopeptidase-like 2; zinc metallopeptidase	XM_425737	
GgaAffx.8173.1.S1_at	0.0145	LOC418129	ENSGALT00000021057	similar to synaptotagmin 10	XM_416361	
Gga.4888.1.S1_s_at	0.0146	PTP4A1	BU124448	protein tyrosine phosphatase type IVA, member 1	NM_001008461	gga.4888
GgaAffx.6911.1.A1_at	0.0146		ENSGALT00000017767			
Gga.4038.1.S1_at	0.0151		BU202624	Transcribed locus		gga.4038
Gga.15280.1.S1_s_at	0.0155		CN223021	Finished cDNA, clone ChEST491d14		gga.14583
GgaAffx.22776.2.S1_s_at	0.0155	P20K; EXFABP; EX-FABP	ENSGALT00000014676	quiescence-specific protein	NM_205422	gga.739
Gga.4120.1.S1_at	0.0155	DUSP1	CR387287	dual specificity phosphatase 1	XM_422941	gga.4120
Gga.7088.1.S1_at	0.0165		BX259751	Finished cDNA, clone ChEST695o3		gga.7088
GgaAffx.26392.1.S1_at	0.0165	LOC417627	ENSGALT00000008115	similar to protein phosphatase 1E; partner of PIX 1	XM_415871	
Gga.7283.1.S1_at	0.0165		BU452897	Finished cDNA, clone ChEST462c20		gga.7283
Gga.8506.1.S2_s_at	0.017	TRIB2; TRB2	BU410444	tribbles homolog 2 (Drosophila)	NM_204401	gga.8506
GgaAffx.4097.1.S1_at	0.0176	LOC418644	ENSGALT00000010624	similar to Metabotropic glutamate receptor 3 precursor	XM_416842	
Gga.571.1.S1_at	0.0176	NR5A1; SF-1; Ad4BP	NM_205077	nuclear receptor subfamily 5, group A, member 1	NM_205077	gga.571
Gga.17278.1.S1_at	0.018	ANKRD43	BU294824	ankyrin repeat domain 43	XM_414649	gga.17278
Gga.16331.1.S1_at	0.018		BU339029	Finished cDNA, clone ChEST209l4		gga.16331
GgaAffx.21237.1.S1_at	0.018		CR523378	Finished cDNA, clone ChEST576k23		gga.20704
GgaAffx.7307.1.S1_at	0.0185	LOC424227	ENSGALT00000018803	similar to 25-hydroxyvitamin D-1 alpha hydroxylase, mitochondrial precursor (Calcidiol 1-monooxygenase) (25-OHD-1 alpha-hydroxylase) (25-hydroxyvitamin D(3) 1-alpha-hydroxylase) (VD3 1A hydroxylase) (P450C1 alpha)	XM_422077	gga.10648
Gga.10041.1.S1_a_at	0.0188	PNOC	BU392271	prepronociceptin	XM_420026	gga.10041
GgaAffx.5888.1.S1_at	0.0188	LOC423252	ENSGALT00000015206	similar to zinc finger, FYVE domain containing 1 isoform 1; tandem FYVE fingers-1 protein; zinc finger protein, subfamily 2A, member 1; double FYVE-containing protein 1; phosphoinositide-binding protein SR3; zinc finger protein,	XM_421172	
GgaAffx.2936.1.S1_at	0.0188	LOC415774	ENSGALT00000007532	similar to system asc amino acid transporter Asc-1	XM_414136	
GgaAffx.22126.1.S1_at	0.019	LOC419762	ENSGALT00000011374	similar to immunoglobulin superfamily, member 4A isoform a; immunosuperfamily protein BI2	XM_417901	gga.5291
GgaAffx.10913.1.S1_at	0.019	LOC428074	ENSGALT00000027529	similar to stomatin-like 3; erythrocyte band 7 integral membrane protein; protein 7.2B	XM_425632	
Gga.2396.1.S1_at	0.0195	BTG1	NM_205350	B-cell translocation gene 1, anti-proliferative	NM_205350	gga.2396
GgaAffx.21945.1.S1_at	0.0195	LOC416316	ENSGALT00000010386	similar to ubiquitin conjugating enzyme	XM_414633	
Gga.8797.1.S1_at	0.0195		CD764248	Finished cDNA, clone ChEST189k11		gga.8797
GgaAffx.6689.1.S1_at	0.0197	LOC423390	ENSGALT00000017215	similar to RIKEN cDNA 4933401N24	XM_421302	
GgaAffx.22642.1.S1_at	0.0197	SLC39A12	ENSGALT00000014008	solute carrier family 39 (zinc transporter), member 12	XM_418616	gga.13510
Gga.6972.2.S1_at	0.0207		BM426736	Transcribed locus, strongly similar to XP_418110.1 PREDICTED: similar to ABI gene family, member 3 [Gallus		gga.6972
Gga.4737.1.S1_at	0.0207	LOC415296	BU119431	actin, cytoplasmic, type 5	NM_001007824	gga.4520
Gga.5058.1.S1_s_at	0.0207	CST3	NM_205500	cystatin C (amyloid angiopathy and cerebral hemorrhage)	NM_205500	gga.5058
Gga.13363.1.S1_at	0.0212	LOC421483	CR353569	C21orf19-like protein	XM_419531	gga.13363
Gga.12437.2.S1_at	0.0214	LOC423420	BU118220	similar to chromogranin A precursor - mouse	XM_421330	

Supplementary Table 3

Affymetrix ID	P-value	Gene Symbol	Accession	Description	RefSeq	UniGene
Gga.11323.1.S1_at	0.0214	CRH	AJ621492	corticotropin releasing hormone	XM_418279	gga.11323
GgaAffx.20609.1.S1_s_at	0.0214		CR524006	Finished cDNA, clone ChEST701p4		gga.9871
Gga.9122.1.S1_at	0.0216		CF253290	Transcribed locus		gga.9122
GgaAffx.4102.1.S1_at	0.0227		ENSGALT00000010639			
GgaAffx.10053.1.S1_at	0.0227	LOC421816	ENSGALT00000025446	similar to ACY1L2 protein	XM_419840	
Gga.13507.1.S1_at	0.0227		CR385142	Finished cDNA, clone ChEST406g11		gga.13507
GgaAffx.20301.1.S1_at	0.0227		CR524314	Finished cDNA, clone ChEST819a3		gga.20550
Gga.1980.1.S1_s_at	0.0232	THBS4	BU388187	thrombospondin 4	XM_424763	gga.1980
Gga.11835.1.S1_at	0.0246	LOC419492	BU118597	similar to AGPA3119	XM_417647	gga.11835
GgaAffx.4634.4.S1_at	0.0247	LOC416083	ENSGALT00000012023	similar to MAGI1c alpha beta2 gamma	XM_414418	
GgaAffx.25755.1.S1_s_at	0.0254	LOC416815	ENSGALT00000004933	similar to silencing mediator of retinoic acid and thyroid hormone receptor extended isoform	XM_415107	
Gga.1840.1.S2_at	0.0257	NEUROD1; NEUROD	BU199562	neurogenic differentiation 1	NM_204920	gga.1840
Gga.12904.1.S1_at	0.0258	LOC416438	BX950566	similar to Neuronal pentraxin II precursor (NP-II) (NP2)	XM_414750	gga.12904
Gga.8081.1.S1_at	0.0264	FSTL4	NM_204502	follistatin-like 4	NM_204502	gga.8081
GgaAffx.4468.2.S1_s_at	0.0274	LOC416068	ENSGALT00000011554	similar to Acyl-coenzyme A oxidase 2, peroxisomal (Branched-chain acyl-CoA oxidase) (BRCACox) (Trihydroxycoprostanoyl-CoA oxidase) (THCCox) (THCA-	XM_414406	
Gga.7020.1.S1_at	0.0274		BU349489	Finished cDNA, clone ChEST299j12		gga.7020
GgaAffx.21710.1.S1_s_at	0.0276	IFRD1; IFR1	CR522905	interferon-related developmental regulator 1	NM_001001468	gga.2458
Gga.2200.1.S1_at	0.0276	CYR61	J04496	cysteine-rich, angiogenic inducer, 61	NM_001031563	gga.2200
GgaAffx.3409.1.S1_at	0.0282	LOC428401	ENSGALT00000008721	similar to hypothetical protein LOC259173 isoform 1	XM_425962	
Gga.15700.1.S1_at	0.0285		BU144794	Finished cDNA, clone ChEST258o16		gga.15700
Gga.2353.1.S1_at	0.0285	TIPARP	BU123098	TCDD-inducible poly(ADP-ribose) polymerase	XM_422828	gga.2353
GgaAffx.3860.2.S1_s_at	0.0285	LOC428711	ENSGALT00000009987	similar to four and a half LIM domains 1 protein, isoform C	XM_426269	
GgaAffx.10313.1.S1_at	0.0285	LOC428381	ENSGALT00000026044	similar to G protein-coupled receptor 20; G protein-coupled receptor 5-1	XM_425941	
GgaAffx.3458.1.S1_s_at	0.0291	DPYD	ENSGALT00000008842	dihydropyrimidine dehydrogenase	XM_426639	gga.20542
Gga.3950.1.S1_at	0.0315	BMP2	NM_204358	bone morphogenetic protein 2	NM_204358	gga.3950
GgaAffx.6812.1.S1_at	0.032	LOC429108	ENSGALT00000017540	similar to thioesterase, adipose associated isoform BFIT2; brown fat inducible thioesterase; START domain containing 14; thioesterase superfamily member 1	XM_426664	
GgaAffx.25940.1.S1_at	0.0339	LOC423677	ENSGALT00000005844	similar to Bifunctional 3-phosphoadenosine 5-phosphosulfate synthethase 2 (PAPS synthethase 2) (PAPSS 2) (Sulfurylase kinase 2) (SK2) (SK 2)	XM_421557	
GgaAffx.24643.1.S1_at	0.0339	LOC421766	ENSGALT00000024672	similar to Sestrin 1 (p53-regulated protein PA26)	XM_419796	
Gga.1750.1.S1_at	0.0339		BU315258	Finished cDNA, clone ChEST147b19		gga.1750
GgaAffx.6904.1.S1_s_at	0.0339	LOC428753	ENSGALT00000017742	similar to protein kinase, cGMP-dependent, type II; cGKII	XM_426309	
Gga.7979.1.S1_at	0.034		BX270512	Transcribed locus, strongly similar to XP_418130.1 PREDICTED: similar to Vesicle amine transport protein 1 homolog (T californica) [Gallus gallus]		gga.7979
GgaAffx.11584.1.S1_s_at	0.034	LOC420846	AJ719481	similar to Hypothetical protein MGC75808	NM_001012863	gga.9773
Gga.6002.1.S1_a_at	0.034	DNMT3A	BU201511	DNA (cytosine-5)-methyltransferase 3A	NM_001024832	gga.6002

Supplementary Table 3

Affymetrix ID	P-value	Gene Symbol	Accession	Description	RefSeq	UniGene
GgaAffx.1849.2.S1_s_at	0.0345	LOC416208, STC2	ENSGALT00000004562	similar to stanniocalcin	XM_414534	
Gga.2166.1.S1_at	0.0345		BU376245	Finished cDNA, clone ChEST732g16		gga.2166
Gga.11766.2.S1_a_at	0.0345	NDP	BX935162	Norrie disease (pseudoglioma)	XM_416765	gga.11766
Gga.5095.1.S1_at	0.0345	CHRNA3	M37336	cholinergic receptor, nicotinic, alpha polypeptide 3	NM_204416	gga.5095
Gga.4922.1.S2_at	0.0348	EGR1	NM_204136	early growth response 1	NM_204136	gga.4922
Gga.19368.1.S1_at	0.0348		CR406662	Finished cDNA, clone ChEST290o16		gga.19368
GgaAffx.8374.1.S1_s_at	0.0359	LOC418190	ENSGALT00000021500	similar to organic anion transporting polypeptide 1a2 variant	XM_416421	
GgaAffx.12984.1.S1_s_at	0.036	SNX3	AJ720881	sorting nexin 3	NM_001006408	gga.15744
GgaAffx.21555.1.S1_s_at	0.0361	LOC420944	CR523060	similar to PSST739	XM_419028	gga.11980
Gga.10364.1.S1_at	0.0361	LOC422064	BX934281	similar to dJ402H5.2 (novel protein similar to worm and fly proteins)	XM_420069	gga.10364
GgaAffx.25620.1.S1_s_at	0.0361	AHCYL1	ENSGALT00000000438	S-adenosylhomocysteine hydrolase-like 1	NM_001030913	gga.5821
Gga.7640.2.S1_at	0.0365	NXT2	BU342317	Nuclear transport factor 2-like export factor 2	NM_001006436	gga.3568
GgaAffx.4941.1.S1_at	0.0369	LOC423158	ENSGALT00000012806	similar to ELGC699	XM_421084	
Gga.2105.1.S1_at	0.0376	M-RIP	BU435267	myosin phosphatase-Rho interacting protein	XM_414806	gga.20857
Gga.16273.1.S1_at	0.0376		BU141803	Finished cDNA, clone ChEST118g23		gga.16273
GgaAffx.5015.1.S1_at	0.0376	ITGA11	ENSGALT00000012998	integrin, alpha 11	XM_413930	
Gga.3676.1.S1_at	0.0378	LOC423952	AJ441642	N-acetylgalactosamine 4-sulfate 6-O-sulfotransferase	XM_421811	gga.3676
Gga.12183.3.S1_s_at	0.0388	LOC428007	BX934631	similar to dehydrogenase/reductase (SDR family) X-linked; dehydrogenase/reductase (SDR family) X chromosome	XM_425577	
Gga.1014.1.S1_at	0.0394		CD732610	Clone C1 putative apoptosis associated protein mRNA, 3' UTR sequence		gga.1014
Gga.2827.2.S1_a_at	0.0394	TIMP3; IMP-3	CR386544	TIMP metallopeptidase inhibitor 3 (Sorsby fundus dystrophy, pseudoinflammatory)	NM_205487	gga.2827
Gga.12811.1.S1_at	0.0411	NUAK2; 1200013B22RIK	BX950299	NUAK family, SNF1-like kinase, 2	XM_417962	gga.12811
Gga.520.1.S1_at	0.0412	LOC396126	AF055478	activin beta B	NM_205206	gga.520
Gga.3640.1.S1_at	0.0412	LOC396335	NM_205376	kinectin	NM_205376	gga.3640
GgaAffx.21459.1.S1_s_at	0.0412		CR523156	Finished cDNA, clone ChEST1028m18		gga.18074
Gga.20018.1.S1_at	0.0412		BU290246	thrombomucin		gga.20018
Gga.3575.1.S1_at	0.0412	LOC422926	BX950350	similar to Gag-Pol polyprotein	XM_420865	gga.3575
GgaAffx.24012.1.S1_at	0.0412	LOC418109	ENSGALT00000020949	similar to Cystine/glutamate transporter (Amino acid transport system xc-) (xCT) (Calcium channel blocker resistance protein CCBR1)	XM_416343	
GgaAffx.5182.1.S1_at	0.0412	LOC431262	ENSGALT00000013361	similar to feminization 1 homolog a	XM_428816	
Gga.261.3.S1_a_at	0.0412	PRLR; PRL-R	AF051808	prolactin receptor	NM_204854	gga.261
Gga.19107.1.S1_at	0.0423		CR406474	Finished cDNA, clone ChEST959a8		gga.19107
GgaAffx.5983.1.S1_at	0.0423	LOC423936	ENSGALT00000015465	similar to arginine-tRNA-protein transferase 1-2p; ATE1-2p	XM_421796	
GgaAffx.26575.1.S1_at	0.0429		ENSGALT00000009181	SEC31-like 2 (S. cerevisiae)	XM_421637	gga.22925
GgaAffx.4754.1.S1_s_at	0.045	SLIT1	ENSGALT00000012327	slit homolog 1 (Drosophila)	XM_421715	gga.2156
Gga.17110.1.S1_at	0.0458		CR391266	Finished cDNA, clone ChEST701k15		gga.17110
GgaAffx.21308.1.S1_s_at	0.0461		CR523307	Finished cDNA, clone ChEST858c10		gga.5874
Gga.2182.1.S1_at	0.0461	IGF1R; IGF-1R	NM_205032	insulin-like growth factor 1 receptor	NM_205032	gga.2182
Gga.3624.1.S1_at	0.0468	PDE3B	BU247139	phosphodiesterase 3B, cGMP-inhibited	NM_001031182	gga.3624

Supplementary Table 3

Affymetrix ID	P-value	Gene Symbol	Accession	Description	RefSeq	UniGene
Gga.8052.1.S1_at	0.0469		BX275092	Transcribed locus		gga.8052
GgaAffx.7851.2.S1_s_at	0.0474	LOC423583	ENSGALT00000020239	similar to osteonidogen	XM_421471	
Gga.3986.2.S1_a_at	0.0476	CA2	CN217291	carbonic anhydrase II	NM_205317	gga.3986
Gga.12107.1.S1_s_at	0.0476	GDPD4	CD727469	glycerophosphodiester phosphodiesterase domain	XM_417276	gga.12107
Gga.2070.2.S1_a_at	0.0484	ID4	AY040529	inhibitor of DNA binding 4, dominant negative helix-loop-helix protein	NM_204282	gga.2070
Gga.13798.2.S1_s_at	0.0484	CRYBB2	AY539830	crystallin, beta B2	NM_205175	gga.646
Gga.16263.1.S1_at	0.0485		BU442145	Finished cDNA, clone ChEST532h13		gga.16263
Gga.25.1.S1_at	0.0494	SH3GL2; SH3P4	NM_204530	SH3-domain GRB2-like 2	NM_204530	gga.25

Supplementary Table 4. Probe sequences used in the *in situ* hybridization.

Gene symbol	Probe sequence (sense sequence)
TSHB	5'- GAGTGTGCCTACTGCCTGGCCATCAACACCACCATCTGCGCTGGA -3'
EYA3	5'- CGTTGGAGGCCTTCTCAGCCCACAGAAGAGGGAAGCTCTGCAGCG -3'
DIO2	5'- GATGGTTCAGCCTCAATGAATATCAAGACGGAAATACATTCTGTA -3'
ICER	5'- CTCAGCAACTGGCAGAAGAGGCAACGCGCAAGAGAGAGCTGCGAC -3'
NR4A3	5'- GCAGGAACCTTCGCAGCCCTCCCCGCCTTCTCCTCCCATCAGCAT -3'
CEBPB	5'- GAAGGTGGAGCAGCTCTCTCGGGAGCTGAGCACCCTCAGGAACTT -3'
SOCS3	5'- CGCATCCAGTGCGAGGGCGGCAGCTTCTCTCTGCAGAGCGACCCG -3'
DIO3	5'- CCTACGGCGCCTACTTCGAGCGGCTCTACGTCATCCAGGAGGAGA -3'
CGA	5'- TCTGGGCAAGACACCGAGTAGACTTGTGAATGAGATGGATGGCTG -3'
FSTL4	5'- GGCCACACTCAGACCTGGGGAGGCTGCACCAAGAGGTATCCGGAA -3'
RLN3	5'- ACGGGAGTCTCTGGGTTTGGCAGGAATGTGTTGCAAGTGGGGCTG -3'
STC2	5'- TTCTGAGCCCCGAGAAGAAGACGGGCGAAGCCAGCAAAGCTGCTG -3'
PNOC	5'- TTCGACCTCCTTGTCTGCATCCTGGAGTGCGAAGGCGAACCCGTG -3'
POMC	5'- CGCTGTGCCACAGCCTGCCCGTGGTGCTGGGGCTGCTGCTGTGTC -3'
GHR	5'- CTCTCCACAAGGCCTTGTGCTCAATGCAACTGCACTGCCTGTGCC -3'
OPRL1	5'- CGCTGTGTCTGATGACCTTACCCTTCCAGGGTACAGACACGTTCC -3'
MC4R	5'- GCGAAGGGCCACTCCTCGGGAGGCTGCTATGAACAACTCTTTGTA -3'
CCK	5'- TACGGCGGCATCTGCATCTGCGTGCTCCTCGCTGCGCTGTCGGTG -3'
CRH	5'- AACTCTGCCCGTCCTGCTCCGCATGGGAGAGGAGTACTTCCTGCG -3'
PRLR	5'- CAGACAGTGACTCAGGACGAGGGAGCTGTGATAGCCCTTCTCTGC -3'
EYA1	5'- CCAGGGAGCGCTTACTTGAGGCAGCCCTGGGCTGTCGTGCAGTCT -3'
EYA2	5'- CACTGCCTACCCTCCTCCAGCGCAGCCCTACGGCATACCTTCCTA -3'
EYA4	5'- GAGGGCGGAAGAATAATCCATCACCCCCTCCGGACAGTGACTTGG -3'
SIX1	5'- GCCACCAACAAACCCAACCAGCTCTCCCCCCTGGACGGGAGCAAA -3'
SIX2	5'- GACAGTTCTGGGGAGCTCGGAGGACGAGAAGACGCCGTCAGGGAC -3'
SIX3	5'- CCCGACCACCAGTGTTTCCAGTTTGACAGAAAGAGCCGAGACGGG -3'
SIX6	5'- CTCCAGCCCAGCCGTCAGCCTCTCCAGCAAGGCGGCCACTTCAGC -3'
DACH1	5'- GGGCCGAAGACCTGGCAGCCACCCATCCTCTCATCGAAGCAGCAG -3'
DACH2	5'- AGCCCTTCTCCAGCTCCATCCCTAGAAGACAGTCAGCGGCCTGGG -3'
PAX6	5'- GAGTCCTCCGCAACCTGGCTAGCGAAAAGCAACAGATGGGTGCCG -3'
TSHR	5'- TGTGCAGCCAGGGCACGGAAAGGTGCCCGTCAGCCTTCTGCGAGT -3'
TGFA	5'- CGGTCACACTTCAATGAGTGCCCCGACTCCCACCGGCAGTTCTGC -3'

Supplementary Table 5. Primer sequences used in the Q-PCR.

Gene Symbol	Primer sequence
TSHB	sense: 5'-CGCCGGATTCTGCATGAC-3' antisense: 5'-GTGCACACGTTTTGGGACAG-3'
DIO2	sense: 5'-CCGAACTCCAGTGTAATCCACATAG-3', antisense: 5'-CACACTTGCCACCAACACTCTT-3'
ICER	sense: 5'-AACAGCTGCCACTGGAGACAT-3' antisense: 5'-CCATTACCACTCCCTGAGGTAAGT-3'
EYA3	sense: 5'-ATGAGACCATCATAATTTTCCATTCA-3' antisense: 5'-GAGCCAATCACCAGAGTTGGAT-3'
DIO3	sense: 5'-AGAAGGTGATGTACCAGGGC-3' antisense: 5'-TTACACTTGGATGACCACCG-3'
CEBPB	sense: 5'-GATCTCTTCGCCGAGGACTATAAA-3' antisense: 5'-CGGGTGAGGCTGATGTAGGT-3'
CGA	sense: 5'-TTTCTCCCGGGCCTATCC-3' antisense: 5'-GCTTCCGATGTAATGTTCTTTGG-3'
PER2	sense: 5'-GATTCCTGTCACAGAGACACGAAA-3' antisense: 5'-CGGCGAAGCCTGGTCTT-3'
CRY1	sense: 5'-CTCATGGAGACAATCAGCAATCA-3' antisense: 5'-TTTCCCGGCGCTAATGC-3'
E4BP4	sense: 5'-AACGACGACTGAATGACCTTGTC-3' antisense: 5'-AGCAGCTCGGCCTTCAAA-3'
BMAL1	sense: 5'-ATGCAGCCTTCCCACAACTC-3' antisense: 5'-TCCTTTTTGGGCCACCTTCT-3'
NR1D2	sense: 5'-CCATAGTTGCATTTGGGTGTGT-3' antisense: 5'-CATTTAGCGATGAAGCAACAAAA-3'
DEC1	sense: 5'-CCTGTTGCCCCAGCTGTT-3' antisense: 5'-AAACCAACCCAATGAAATAAACGT-3'
DEC2	sense: 5'-CGCTTCGGTGCATTGCT-3' antisense: 5'-GTAGGCCGCTAAGGTCTGGAA-3'
PER3	sense: 5'-AGCCATTGTGCCTCTAGTGAATTTAC-3' antisense: 5'-GCCAATCCACTGCCTGATG-3'
GAPDH	sense: 5'-AACCCCCAATGTCTCTGTTGTT-3' antisense: 5'-TCACTACCCTCTTGATGTCATCATATT-3'